

1 Spatiotemporal responses in crop water footprint and benchmark 2 under different irrigation techniques to climate change scenarios in 3 China

4 Zhiwei Yue^{1,3,*}, Xiangxiang Ji^{1,3,*}, La Zhuo^{2,3,4,5}, Wei Wang^{4,5}, Zhibin Li^{4,5}, Pute Wu^{2,3,4,5}

5 ¹College of Water Resources and Architectural Engineering, Northwest A&F University, Yangling 712100, China

6 ²Institute of Soil and Water Conservation, Northwest A&F University, Yangling 712100, China

7 ³Institute of Water-saving Agriculture in Arid Regions of China, Northwest A&F University, Yangling 712100, China

8 ⁴Institute of Soil and Water Conservation, Chinese Academy of Sciences and Ministry of Water Resources, Yangling 712100,
9 China

10 ⁵ University of Chinese Academy of Sciences, Beijing 100049, China.

11

12 *The authors contribute equally.

13 Correspondence to: La Zhuo (zhuola@nwafu.edu.cn; lzhuo@ms.iswc.ac.cn) and Pute Wu (gjzwpt@hotmail.com)

14

15 **Abstract.** Adaptation to future climate change with limited water resources is a major global challenge to sustainable and
16 sufficient crop production. However, the large-scale responses of crop water footprint and its associated benchmarks under
17 various irrigation techniques to future climate change scenarios remain unclear. The present study quantified the responses of
18 maize and wheat water footprint per unit yield (WF, m³ t⁻¹) and corresponding WF benchmarks under two representative
19 concentration pathways (RCPs) in the 2030s, 2050s, and 2080s at a 5-arc minute grid level in China. The AquaCrop model
20 with the outputs of six global climate models in Coupled Model Intercomparison Project Phase 5 (CMIP5) as its input data
21 was used to simulate the WF of maize and wheat. The differences among rain-fed and furrow-, micro-, and sprinkler-irrigated
22 wheat and maize were identified. Compared with the baseline year (2013), maize WF will increase under both RCP2.6 and
23 RCP8.5, by 17 % and 13 %, respectively, until the 2080s. Wheat WF will increase under RCP2.6 (by 12 % until the 2080s)
24 and decrease by 12 % under RCP8.5 until the 2080s, with a higher increase in wheat yield and decrease in wheat WF due to
25 the higher CO₂ concentration in 2080s under RCP8.5. WF will increase the most for rain-fed crops. Relative to rain-fed crops,
26 micro irrigation and sprinkler irrigation result in the smallest increases in WF for maize and wheat, respectively. These water-
27 saving managements will mitigate the negative impact of climate change more effectively. The WF benchmarks of maize and
28 wheat in the humid zone are 13–32 % higher than those in the arid zone. The differences in WF benchmarks among various
29 irrigation techniques are more significant in the arid zone, which can be as high as 57%, for 20th percentile WF benchmarks
30 of sprinkler-irrigated and micro-irrigated wheat. Nevertheless, WF benchmarks will not respond to climate changes as
31 dramatically as the WF in the same area, especially in the area with limited agricultural development. The present study
32 demonstrated that the visible different responses to climate change in terms of crop water consumption, water use efficiency,
33 and WF benchmarks under different irrigation techniques cannot be ignored. It also lays the foundation for future investigations
34 into the influences of irrigation methods, RCPs, and crop types on WF and its benchmarks in response to climate change in all
35 agricultural regions worldwide.

36 **1 Introduction**

37 The progressive decline in water resource availability is a major impediment to global food production security (Pastor
38 et al., 2019; Trnka et al., 2019; Konapala et al., 2020). Food crops are the main source of human nutrition (Myers et al., 2017;
39 Lobell and Gourdj, 2012). Humans depend on food crops for ~47 % of their daily protein intake (FAO, 2021). However, as a
40 result of human activity, the climate system is changing and global warming is a significant characteristic of this process (IPCC,
41 2021). Since the 1980s, each successive decade has been warmer than any preceding one after 1850 (Kappelle, 2020). Climate
42 change affects water consumption and crop yield by altering precipitation, temperature, carbon dioxide (CO₂) concentration,
43 and other factors during crop growth (Hatfield and Dold, 2019). Crop adaptation to future climate change with limited water
44 resources has become a major challenge in sustainable crop production and supply worldwide.

45 The water footprint per unit crop (WF, m³ t⁻¹) (Hoekstra, 2003) is the amount of water consumed by the crop per unit
46 yield during crop growth within a certain region. It includes blue WF (surface and groundwater), green WF (precipitation that
47 will not become runoff), and grey WF (freshwater that assimilates pollutants from human activities) (Hoekstra et al., 2011).
48 Blue and green WF are collectively known as consumptive WF, and grey WF is also called degradative WF (Hoekstra, 2013).
49 Unlike traditional crop water productivity and other agricultural water metrics, WF covers water consumption, sources, and
50 spatiotemporal dimensions during the crop growth period. Therefore, water consumption intensity and efficiency for irrigated
51 and rain-fed planting modes may be compared. WF is an effective indicator of the sustainability of regional water use and
52 optimal water resource allocation (Xu et al., 2019; Mali et al., 2021). The present study focuses exclusively on consumptive
53 WF, which depends on crop yield and the intensity of water consumption per unit planted area.

54 Several studies have been conducted on the responses of WF to future climate change. Nevertheless, no consensus has
55 been reached. Certain scholars believe that future climate change will weaken food crop production security. Ahmadi et al.
56 (2021) reported that maize WF in the Qazvin Plain of India will increase by 42 % and 147 % under representative concentration
57 pathways (RCP) 4.5 and RCP8.5, respectively, by 2061–2080. Zheng et al. (2020) found that rice yield in Henan and Jiangsu
58 Provinces (China) will decrease, while WF will increase under four RCPs at various stages of the 21st century. Other scholars
59 believe that crop yield may actually benefit from future increases in precipitation and atmospheric CO₂ concentration. Jans et
60 al. (2021) considered the combined effects of changes in climatic factors, such as temperature, precipitation, and rising
61 atmospheric CO₂ concentration, and predicted that between 2011 and 2099, global cotton yield will increase by > 50 % and
62 WF will decrease by 30 % under RCP8.5. Arunrat et al. (2020) found that in the present century, the yield of individual and
63 large-scale rice farms in Thailand will increase by 1–30 % and 2–31 %, respectively, while WF will decrease by 10–43 % and
64 1–67 %, respectively, under RCP4.5. Significant spatiotemporal differences in WF under various irrigation techniques have
65 been confirmed at the site (Chukalla et al., 2015) and regional (Wang et al., 2019) scales. However, current large-scale studies
66 on the responses of WF to environmental change are usually based on simulations assuming adequate furrow irrigation. These
67 studies exclude comparisons between various irrigation techniques and the differences in their influences on crop WFs.

68 Although Dai et al. (2020) optimised maize and wheat cropping patterns under RCP4.5 and RCP8.5 with consideration of
69 various irrigation modes in the Huaihe River Basin in China by 2050, they only considered blue water.

70 Magnitudes and constitution of crop WF vary widely among regions and areas (Mekonnen and Hoekstra, 2011). To
71 encourage water users to reduce WF to a reasonable level, Hoekstra (2013, 2014) recommended establishing WF benchmarks
72 for different products as they facilitate prudent water allocation and fair water resource sharing among sectors and users
73 (Hoekstra, 2013). On the large-scale, specific WF benchmarks can be set for crops grown on different farms within the same
74 region (Mekonnen and Hoekstra, 2014). A previous study demonstrated the sensitivity of WF benchmarks to climate zones
75 (Zhuo et al., 2016a). WF benchmarks significantly differ among irrigation techniques, especially in arid zones (Wang et al.,
76 2019). However, little is known about the responses of WF benchmarks under different irrigation techniques to future climate
77 change.

78 To investigate the influence of future climate change on large-scale WF and benchmarks under diverse irrigation
79 techniques, maize and wheat grown in mainland China were the subjects of this study. We used the outputs of six global
80 climate models (GCMs) (Table 1), including three models each for relatively wet and dry climate outputs, in Coupled Model
81 Intercomparison Project Phase 5 (CMIP5). We then used the AquaCrop model to simulate the spatiotemporal responses of
82 blue and green WF and corresponding WF benchmarks for wheat and maize in the 2030s (2020–2049), 2050s (2040–2069),
83 and 2080s (2070–2099) under RCP2.6 and RCP8.5 at a 5-arc minute grid resolution. We distinguished between rain-fed and
84 irrigated planting modes and among furrow, micro, and sprinkler irrigation.

85 As of 2019, China was the world's second largest maize and largest wheat producer, accounting for 23 % and 17 % of
86 total global production, respectively (FAO, 2021). China's cereal production has helped stabilise global food production and
87 supply. In 2019, the planted areas of maize and wheat in China were 41 million ha and 24 million ha, respectively, and
88 accounted for 25 % and 14 % of the national total croplands, respectively (NBSC, 2021). Cereal production consumes
89 substantial volumes of water in China, and these quantities change over time. Zhuo et al. (2019) reported that maize water
90 consumption increased by 49 % between 2000 and 2013 as planted areas and feed demand increased. Conversely, Wang et al.
91 (2019) reported that wheat planted and irrigated areas decreased and water consumption slightly declined (4.4 %) from 2000
92 to 2014. Other studies reported that maize and wheat consume relatively more water in the North than the South of China (Tian
93 et al., 2019; Wang et al., 2019). Developing water-saving irrigation has become an important way to alleviate the prominent
94 contradiction between water resources utilization and grain production in China. According to NBSC (2021), the area of water-
95 saving irrigation projects in China in 2019 was 37 million ha, including 7 million ha for micro irrigation. Therefore, micro
96 irrigation does apply to food crops in China despite the limited irrigated area. For instance, in Xinjiang province, the area of
97 micro irrigated maize and wheat was 0.033 million ha in 2009 (CIDDC, 2022), of which the wheat area dominated at up to
98 0.031 million ha (Wang et al., 2011). Meanwhile, some scholars are conducting research on micro irrigated maize (Bai and
99 Gao, 2021; Guo et al., 2021) and wheat (Li et al., 2021; Zain et al., 2021) in China, especially in the North. Therefore, the
100 water consumption rates of these staple crops under future climate change scenarios with different irrigation techniques should
101 be closely monitored to ensure water supply and food crop production security in China and worldwide. Compared to existing

102 literatures, the innovations of the current research are embodied in two points. The present study clarifies large-scale
103 spatiotemporal responses of WF to future climate change scenarios under different irrigation techniques for the first time. This
104 analysis is also the first to explore large-scale changes in WF benchmarks under future climate change scenarios.

105

106 **Table 1.** Inventory of global climate models (GCMs) used in the current study.

GCM	Institute	Reference	Type
CCCMA- CanESM2	Canadian Centre for Climate Modelling and Analysis	Arora et al. (2011); von Salzen et al. (2013)	Wet
CESM1- CAM5	National Science Foundation, Department of Energy, National Center for Atmospheric Research	Hurrell et al. (2013)	
GFDL-CM3	NOAA Geophysical Fluid Dynamics Laboratory	Delworth et al. (2006); Donner et al. (2011)	
FIO-ESM	The First Institute of Oceanography, State Oceanic Administration, China	Qiao et al. (2013)	Dry
GISS-E2R	NASA Goddard Institute for Space Studies USA	Schmidt et al. (2006); Schmidt et al. (2014)	
IPSL-CM5A- MR	Institute Pierre Simon Laplace	Dufresne et al. (2013)	

107

108 **2 Method and data**

109 **2.1 Research set-up**

110 We studied the spatiotemporal responses of blue and green WF and corresponding WF benchmarks for two crops (maize
111 and wheat) to future climate change under two climate change scenarios (RCP2.6 and RCP8.5) using four different planting
112 modes (rain-fed and furrow-, micro-, and sprinkler-irrigated). First, we determined the baseline year. Second, we considered
113 different planting modes to quantify WF and corresponding WF benchmarks of two crops in the baseline year and future year
114 levels under two climate change scenarios. Finally, the spatiotemporal responses of crop WF and corresponding WF
115 benchmarks to future climate change were analysed (Fig. 1).

116

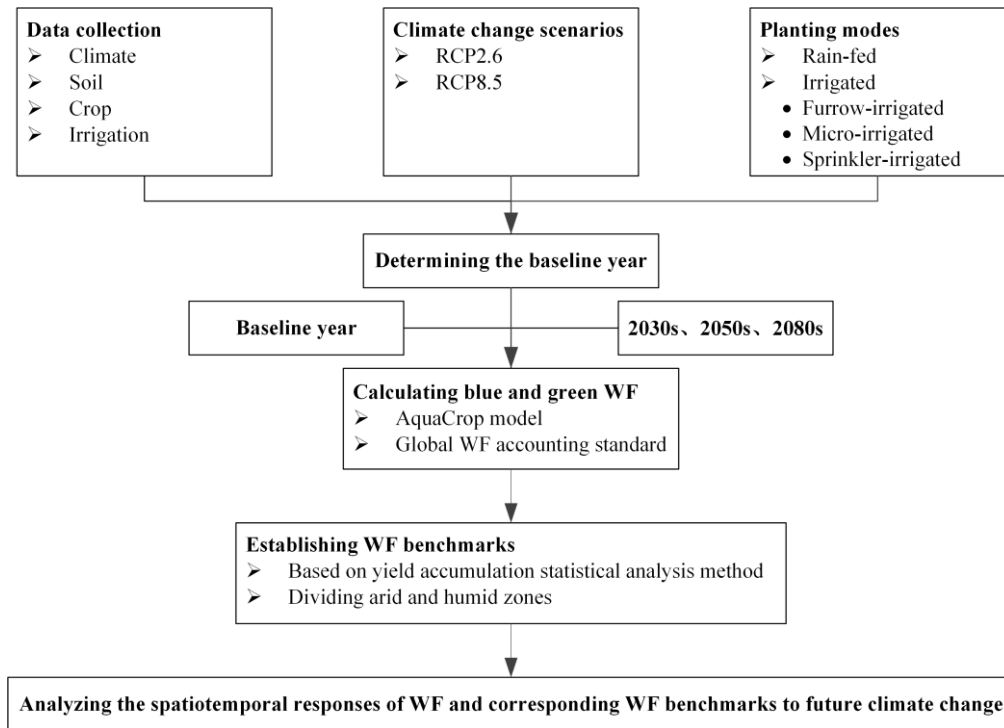


Figure 1. Flow chart for the study.

117
118
119

120 2.2 Determining the baseline year

121 To ensure that the simulation results of future climate change scenarios are still reliable and meaningful, the baseline year
122 was determined. Climate determines the annual variability of WF (Zhuo et al., 2014), and the baseline year should be
123 determined when there is a relative balance between aridity and moisture. Hence, the aridity index (AI) was used here. Annual
124 reference evapotranspiration (ET_0 , mm) and precipitation (PR, mm) in China were calculated (Harris et al., 2014). Then, the
125 AI was calculated, and climate change trends from 2000 to 2014 were analysed. The year 2013 was designated the baseline as
126 its drought level was nearest the 15-year national average. The AI was calculated according to the method of Middleton and
127 Thomas (1997):

$$AI = \frac{PR}{ET_0}, \quad (1)$$

128 2.3 Water footprint per unit crop calculation

129 WF ($m^3 t^{-1}$) comprises blue WF (WF_b , $m^3 t^{-1}$) and green WF (WF_g , $m^3 t^{-1}$):

$$WF = WF_b + WF_g, \quad (2)$$

130 where WF_b and WF_g were calculated as the quotient of the blue (CWU_b , $m^3 ha^{-1}$) and green (CWU_g , $m^3 ha^{-1}$) components of
 131 crop water use (CWU , $m^3 ha^{-1}$) and crop yield (Y , $t ha^{-1}$), respectively. CWU_b and CWU_g were equivalent to the cumulation
 132 of daily evapotranspiration (ET , $mm d^{-1}$) throughout the whole crop growth period (Hoekstra et al., 2011):

$$WF_b = \frac{CWU_b}{Y} = \frac{10 \times \sum_{d=1}^{lgp} ET_b}{Y}, \quad (3)$$

$$WF_g = \frac{CWU_g}{Y} = \frac{10 \times \sum_{d=1}^{lgp} ET_g}{Y}, \quad (4)$$

133 where ET_b and ET_g (mm) refer to the blue and green water evapotranspiration, respectively, and lgp refers to the number of
 134 days of the crop growth period. The coefficient, 10, is a unit conversion factor, transforming the water depth of ET (mm) into
 135 the water amount per unit land area of CWU ($m^3 ha^{-1}$).

136 The ET and Y per grid for each crop were simulated by the AquaCrop model based on the dynamic daily soil water
 137 balance (Mekonnen and Hoekstra, 2010):

$$S_{[t]} = S_{[t-1]} + PR_{[t]} + IRR_{[t]} + CR_{[t]} - ET_{[t]} - RO_{[t]} - DP_{[t]}, \quad (5)$$

138 where $S_{[t]}$ and $S_{[t-1]}$ (mm) refer to the water content in soil when the day, t , ends and begins, respectively; $PR_{[t]}$ (mm) is the
 139 amount of precipitation on day, t ; $IRR_{[t]}$ (mm) is the amount of water used for irrigation; $CR_{[t]}$ (mm) is the capillary rise to the
 140 crop root zone from the shallow groundwater; $RO_{[t]}$ (mm) is the water lost by surface runoff due to precipitation; and $DP_{[t]}$
 141 (mm) is the water lost by deep percolation caused by excessive precipitation or irrigation. It was assumed that $CR_{[t]} = 0$ as the
 142 ground water depth was $\gg 1$ m (Allen et al., 1998). $RO_{[t]}$ was calculated using the Soil Conservation Service curve-number
 143 (CN) equation (USDA, 1964; Rallison, 1980):

$$RO_{[t]} = \frac{(PR_{[t]} - I_a)^2}{PR_{[t]} + S - I_a}, \quad (6)$$

$$S = 254 \left(\frac{100}{CN} - 1 \right), \quad (7)$$

144 where S (mm) is the potential maximum water storage, and I_a (mm) is the initial amount of water loss before the runoff
 145 formation.

146 By tracking the daily flow of water in and out of the crop root zone, we separated the daily blue and green soil water
 147 balances (Zhuo et al., 2016b):

$$S_{b[t]} = S_{b[t-1]} + (PR_{[t]} + IRR_{[t]} - RO_{[t]}) \times \frac{IRR_{[t]}}{PR_{[t]} + IRR_{[t]}} - (DP_{[t]} + ET_{[t]}) \times \frac{S_{b[t-1]}}{S_{[t-1]}}, \quad (8)$$

$$S_{g[t]} = S_{g[t-1]} + (PR_{[t]} + IRR_{[t]} - RO_{[t]}) \times \frac{PR_{[t]}}{PR_{[t]} + IRR_{[t]}} - (DP_{[t]} + ET_{[t]}) \times \frac{S_{g[t-1]}}{S_{[t-1]}}, \quad (9)$$

148 where $S_{b[t]}$ and $S_{b[t-1]}$ (mm) are the blue water content in soil when the day, t , ends and begins, respectively; and $S_{g[t]}$ and $S_{g[t-1]}$
 149 (mm) are the green water content in soil when the day, t , ends and begins, respectively. It is assumed that the initial soil water
 150 content before the crop growth period is green water.

151 In AquaCrop, the daily transpiration ($Tr_{[t]}$, mm) calculates the daily shoot biomass production (B , kg) using the normalised
 152 crop biomass water productivity (WP^* , $kg m^{-2}$) (Raes et al., 2017):

$$B = WP^* \times \sum \frac{Tr_{[t]}}{ET_{0[t]}}, \quad (10)$$

153 where WP^* is normalised to consider CO_2 concentration, reference evapotranspiration (ET_0), and crop classes (C3 or C4) so
 154 that it is applicable to various locations and seasons. Water productivity remains constant for specific crops. Y , as the
 155 harvestable portion of final B , is calculated by multiplying B with the adjusted reference Harvest Index (HI_0 , %):

$$Y = f_{HI} \times HI_0 \times B, \quad (11)$$

156 where f_{HI} is a correction factor for HI_0 . It considers the water and temperature stresses during the crop growth period. Being
 157 consistent with the existing widely used calibration method (Mekonnen and Hoekstra, 2011; Zhuo et al., 2016b, 2016c, 2019;
 158 Wang et al., 2019; Mialyk et al., 2022), the simulated Y per grid for each crop in 2013 was validated via scaling model
 159 simulation outputs to correspond with the crop yield statistics data at the provincial level (NBSC, 2021). With the consistent
 160 crop parameters and calibrated scaling factors for the Y simulation which represent the existing agricultural production level,
 161 climate was the only variable for future scenario simulations.

162 In the simulation, different planting modes, namely rain-fed and three different irrigation techniques (furrow, micro, and
 163 sprinkler irrigation), were considered. The irrigation schedule of three irrigation techniques in the model was the Generation
 164 of Irrigation Schedule, namely the generation of an irrigation schedule by specifying a time and depth criterion for planning
 165 or evaluating a potential irrigation strategy. Table S6 shows the parameters of three irrigation techniques (Raes et al., 2017).
 166 We can adjust the simulated ET and Y according to the performance of the irrigation schedule.

167 **2.4 Benchmarking consumptive WF in crop production**

168 Based on the work of Mekonnen and Hoekstra (2014), we ranked grid-level WF for each crop in ascending order of size
 169 against the corresponding cumulative percentages of the total crop production. The annual WF of 20 % or 25 % of the producers
 170 with the highest water productivity in China was set as the annual WF benchmark. The climate zones should be divided when
 171 WF benchmarks are established (Zhuo et al., 2016a). To this end, the AI partitioned China into arid (< 0.5) and humid (> 0.5)
 172 zones based on the annual ET_0 and PR from 2000 to 2014 at a 30-arc minute grid resolution (Harris et al., 2014) (Fig. 2).

173



174
175 **Figure 2.** Regions and climate zones of mainland China.
176

177 **2.5 Data sources**

178 Monthly climate data, such as maximum (T_x), minimum air temperature (T_n), precipitation (PR), and reference
179 evapotranspiration (ET_0), from 2000 to 2014 at a resolution of 30-arc minute were derived from the CRU-TS 3.24 dataset
180 (Harris et al., 2014; CEDA, 2018). The mean annual atmospheric CO_2 concentration (ppm) from 2000 to 2014 was obtained
181 from the Mauna Loa Observatory, Hawaii, USA (NOAA, 2018). The downscaled outputs of six GCMs at a 5-arc minute grid
182 resolution in the 2030s, 2050s, and 2080s were obtained from the Climate Change, Agriculture and Food Security (CCAFS)
183 database (Navarro-Racines et al., 2020; CCAFS, 2015). As the CCAFS database has no ET_0 data, we calculated ET_0 for each
184 climate scenario using temperature inputs via the FAO Penman-Monteith method with missing data as described by Allen et
185 al. (1998). The projected CO_2 concentrations under RCP2.6 and RCP8.5 were obtained from van Vuuren et al. (2007) and
186 Riahi et al. (2007), respectively. To make the model simulation more in line with the actual situation in China, we reset the
187 maximum root depth (Z_x) according to the FAO-56 recommendation (Allan et al., 1998). In addition, we further combined the
188 literature research on maize and wheat in China to reset the HI_0 (Zhuo et al., 2016c). The other parameters used in AquaCrop
189 were derived from Raes et al. (2017). Soil texture data and soil water capacity data at a 5-arc minute grid resolution were
190 acquired from the ISRIC Soil and Terrain database (Dijkshoorn et al., 2008) and ISRIC-WISE dataset (Batjes, 2012),
191 respectively. The planted areas for each irrigated or rain-fed crop at a 5-arc minute grid resolution were acquired from the
192 MIRCA2000 dataset (Portmann et al., 2010). We divided these planted areas into different parts subjected to various irrigation

193 techniques using statistical yearbook data (NBSC, 2021). Provincial-level crop yield statistics data were procured from the
194 National Bureau of Statistics of China (NBSC, 2021).

195 **3 Results**

196 **3.1 Future climate change trends in maize and wheat planted areas**

197 In the baseline year 2013, the average annual reference evapotranspiration (ET_0) and precipitation (PR) in the planted
198 areas of two crops were 941 mm and 727 mm, respectively. Compared with the baseline level of 2013, the average annual ET_0
199 and PR in the planted areas of two crops will both increase under two RCPs, and the increase in ET_0 exceeded that of PR. ET_0
200 will increase by 17 % and 29 % under RCP2.6 and RCP8.5, respectively, until the 2080s. However, PR will increase by 8 %
201 and 14 %, respectively. The increases under RCP8.5 (18–29 % and 3–14 % for ET_0 and PR, respectively) were much higher
202 than those under RCP2.6 (16–17 % and 4–8 % for ET_0 and PR, respectively). Climate change will be relatively more intense
203 under RCP8.5. The increases in ET_0 were concentrated from April to August (14–39 mm). The increases in PR were
204 concentrated between June and August (8–20 mm and 12–28 mm, respectively). However, PR will decline in May, July,
205 November, and December, and it will decline more in May (≤ 9 mm until the 2030s) (Fig. 3a, b). Water and heat resources
206 were unevenly distributed in the planted areas of the two crops in 2013. ET_0 was relatively higher in East Coast and North
207 China. PR distribution was comparatively higher in the South and lower in the North (Fig. S4). Compared with 2013, ET_0 and
208 PR for the most heavily planted areas will increase under both scenarios until the 2080s. The areas with a relatively greater
209 increase in ET_0 were distributed mainly in Southwest and Northeast (Fig. 3c, e), and PR increased relatively faster in Northwest
210 and Jing-Jin (Fig. 3d, f). ET_0 decreased mainly in Xinjiang and Inner Mongolia (Fig. 3c, e), and PR decreased mainly in
211 Xinjiang, Tibet, Northeast, and South Coast (Fig. 3d, f). However, the areas where ET_0 decreased were 86–94 % smaller than
212 those where PR decreased.

213

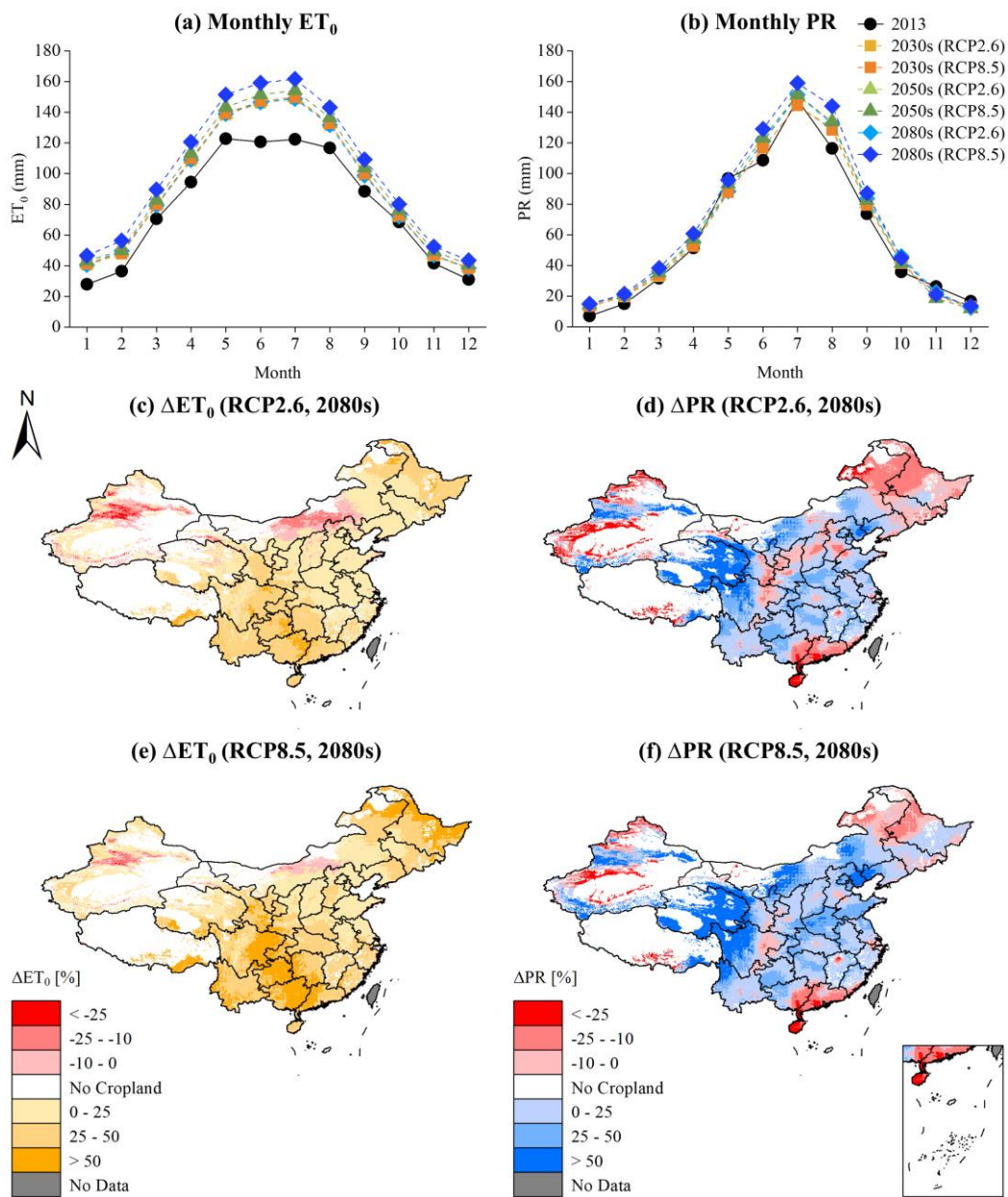


Figure 3. Future climate projections for the maize and wheat planted zones in China.

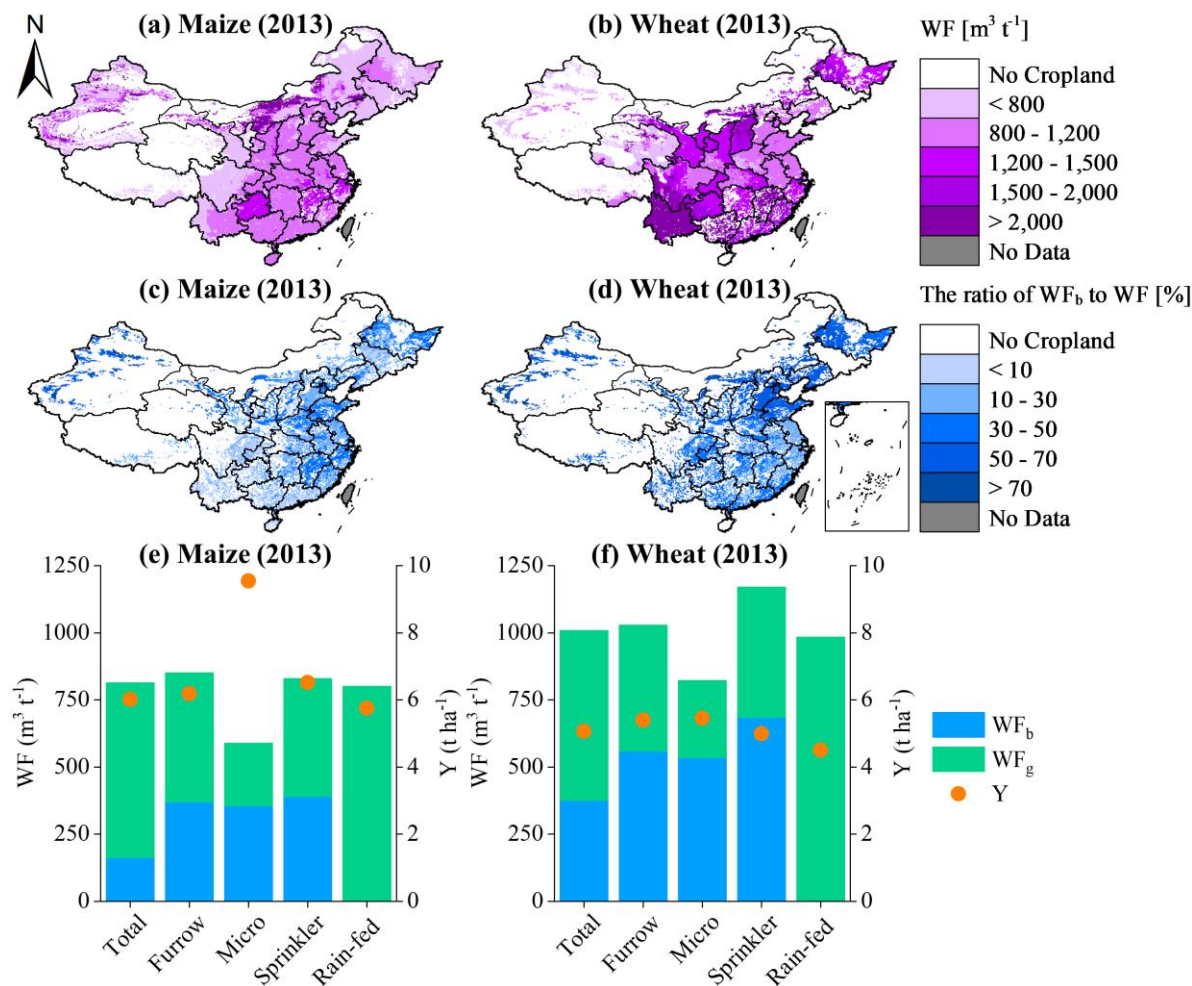
214
215
216

217 3.2 WF distribution in the baseline year 2013

218 The national average WF for wheat ($1,008 \text{ m}^3 \text{ t}^{-1}$) was higher than that for maize ($813 \text{ m}^3 \text{ t}^{-1}$) in the baseline year 2013.
219 The corresponding blue WF proportions were 37 % and 20 %, respectively. The reason for this discrepancy is that maize is a
220 C4 crop while wheat is a C3 crop. C4 crops have a relatively higher CO_2 fixation efficiency and faster photosynthetic rate than

221 C3 crops. Hence, maize can accumulate comparatively more yield than wheat under the same water consumption condition
 222 (Wang et al., 2012). Figure 4 shows that the high WF_g value was mainly distributed in areas with relatively greater precipitation
 223 during crop growth, i.e., abundant green water resources. The main component of WF is WF_g ; therefore, the high maize WF
 224 was mainly distributed in Northwest (Fig. 4a), while the high wheat WF was mainly distributed in Southwest and South Coast
 225 (Fig. 4b). Elevated ET_0 and insufficient precipitation can increase blue water consumption in food production. Thus, the high
 226 WF_b value was mainly distributed in areas with uneven water and heat resource distributions during crop growth. The high
 227 maize WF_b was mainly distributed in Northwest and East Coast (Fig. 4c), while that of wheat was distributed mainly in North
 228 China (Fig. 4d). In all grids, the proportions of WF_b and WF_g were up to 68 % (wheat in Xinjiang) (Table S2) and 98 % (maize
 229 in Hainan) (Table S1), respectively.

230



231

232

233

Figure 4. WF of maize and wheat in China in 2013.

234 A comparison of rain-fed and irrigation techniques demonstrated that the WF of maize and wheat under furrow and
235 sprinkler irrigation was higher than that under rain-fed in 2013. The WF of micro-irrigated crops was lower than that of rain-
236 fed crops. The WF of maize ($850 \text{ m}^3 \text{ t}^{-1}$) and wheat ($1,170 \text{ m}^3 \text{ t}^{-1}$) was highest under furrow and sprinkler irrigation, respectively.
237 For wheat under all three irrigation techniques, WF_b was dominant (54–65 %). However, WF_b for maize was only dominant
238 under micro irrigation (61 %). Micro-irrigated (9.55 t ha^{-1} for maize and 5.46 t ha^{-1} for wheat) and rain-fed (5.76 t ha^{-1} for
239 maize and 4.51 t ha^{-1} for wheat) crops had the highest and lowest yield, respectively, in 2013. The responses of maize yield to
240 rain-fed and various irrigation techniques were stronger than those of wheat yield (Fig. 4e, f).

241 3.3 Spatiotemporal responses of WF to future climate change

242 Compared with the baseline year 2013 and at the national average level, maize WF will increase under both RCP2.6 and
243 RCP8.5, by 17 % and 13 %, respectively, until the 2080s. The WF of wheat will increase under RCP2.6 (by 12 % until the
244 2080s) but decrease by 12 % under RCP8.5 until the 2080s (Fig. 5a). The increases in CO_2 concentration and, by extension,
245 yield gain, will be lower under RCP2.6 than RCP8.5. During the same period, the increases in WF under RCP2.6 will be 1–
246 3 % higher for maize and 2–10 % higher for wheat than those under RCP8.5. There will be relatively smaller differences in
247 CO_2 concentration between climate scenarios of the 2030s (431 ppm under RCP2.6 and 449 ppm under RCP8.5). Thus, the
248 differences in WF between RCPs will be smaller before the 2030s and larger after the 2050s. The WF of irrigated wheat under
249 RCP8.5 will decline by 3 % until the 2050s and by 15 % until the 2080s. The increase in WF will be highest under rain-fed,
250 and the WF of rain-fed maize and wheat under RCP2.6 will increase by 19 % and 24 %, respectively, until the 2080s. By
251 contrast, the WF of irrigated maize and wheat under RCP2.6 will only increase by 13 % and 7 %, respectively, until the 2080s
252 (Fig. 5a). A comparison of the various irrigation techniques demonstrated that the WFs of wheat and maize respond differently
253 under the same scenario. The increase in WF amplitude for maize will be highest under furrow irrigation (14 % and 11 %
254 under RCP2.6 and RCP8.5 until the 2080s, respectively) and lowest under micro irrigation (5 % and 2 % under RCP2.6 and
255 RCP8.5 until the 2080s, respectively). The WF of sprinkler-irrigated wheat under RCP8.5 will decline by 1 % until the 2030s.
256 The WF of wheat under micro irrigation had the highest increase (9 % until the 2080s under RCP2.6) and the lowest decrease
257 (14 % until the 2080s under RCP8.5). The WF of wheat under sprinkler irrigation had the lowest increase (only 2 % until the
258 2080s under RCP2.6) and the highest decrease (19 % until the 2080s under RCP8.5) (Fig. 5b).

259

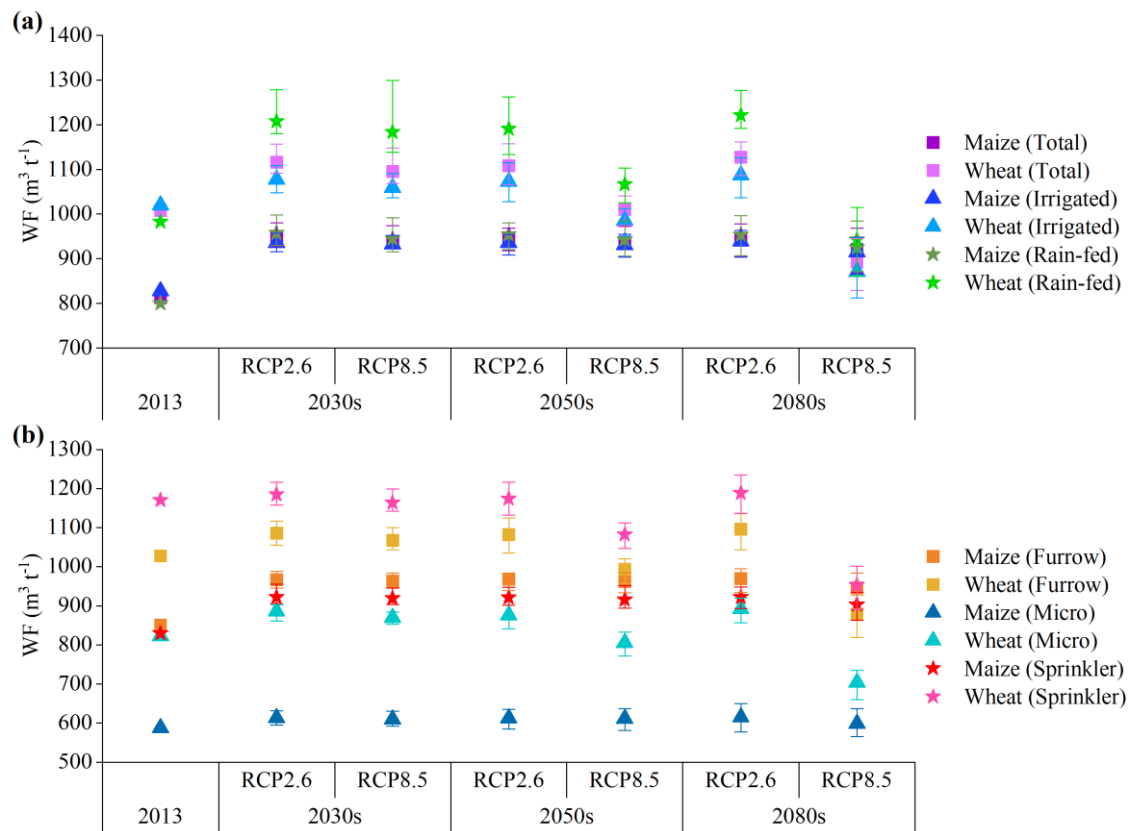


Figure 5. WF of maize and wheat in 2013 and future year levels under various climate change scenarios in China.

260

261

262

263

264

265

266

267

268

269

270

271

272

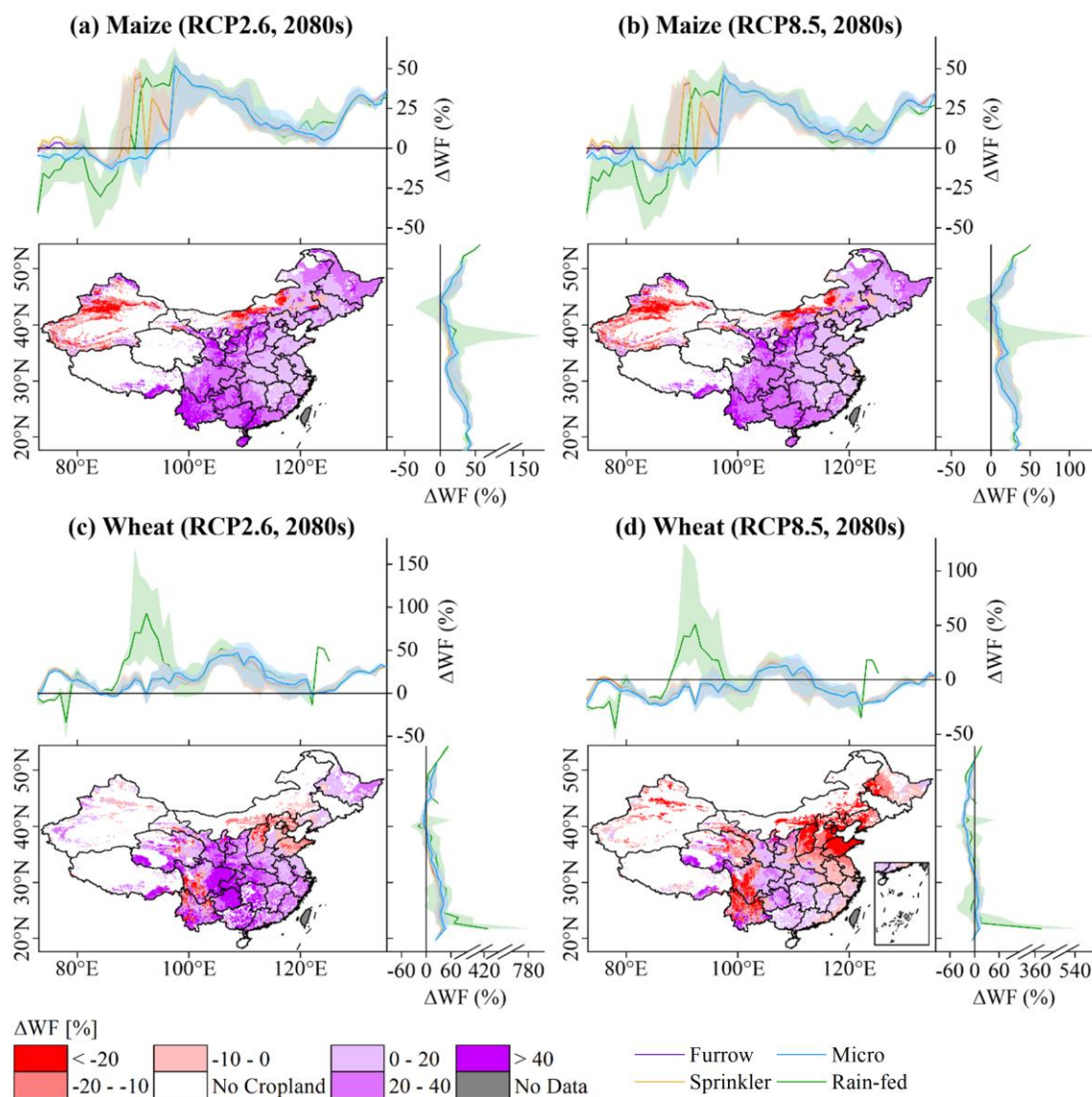
273

274

275

The spatial distribution of the relative changes in maize and wheat WF from 2013 to the 2080s showed regional differences. The WF will increase for 90–93 % of all areas planted with maize (Fig. 6a, b), and it will increase for 78 % of all areas planted with wheat under RCP2.6 (Fig. 6c) and decrease for 81 % of all areas planted with wheat under RCP8.5 (Fig. 6d). Increases in ET_0 lead to increases in WF, while decreases in PR lead to increases in WF_b (Fig. S6). Hence, the regions with relatively greater increases in WF were mainly distributed where ET_0 strongly increased and PR slightly increased or even decreased. In Yunnan, maize WF increased by 44 % and 38 % under RCP2.6 and RCP8.5, respectively. In Guangxi, wheat WF increased by 50 % and 16 % under RCP2.6 and RCP8.5, respectively (Table S5). Comparison of rain-fed and various irrigation techniques revealed that the WF of each crop responded uniquely to latitudinal and longitudinal climate change under the same scenario. The responses of maize WF to climate change with latitude were relatively consistent. It increased by 27–43 % at 19–26 °N and ~51 °N latitude and decreased at ~44 °N latitude. By contrast, the responses of WF for rain-fed maize were more sensitive at ~40 °N and ~52 °N latitude. The responses of maize WF vary widely within 74–100 °E longitude. The WF of maize under rain-fed and furrow and sprinkler irrigation declined at 74–90 °E longitude. The increase in WF for maize under rain-fed at 93–98 °E longitude was 3–51 % higher than the increase in WF for maize under furrow and

276 sprinkler irrigation. The WF of micro-irrigated maize decreased at 74–95 °E longitude (Fig. 6a, b). The responses of wheat
 277 WF to climate change with latitude and longitude were relatively consistent. However, in certain areas, there were large
 278 differences in wheat WF between rain-fed and the three irrigation techniques. The WF of wheat under rain-fed decreased at
 279 74–80 °E longitude and by more than the WF of wheat under the three irrigation techniques at the same longitude range. The
 280 increases in the WF of wheat under rain-fed at ~93 °E and ~122 °E longitude and ~22 °N latitude were significantly higher
 281 than the increases in WF of wheat under the three irrigation techniques (Fig. 6c, d).
 282

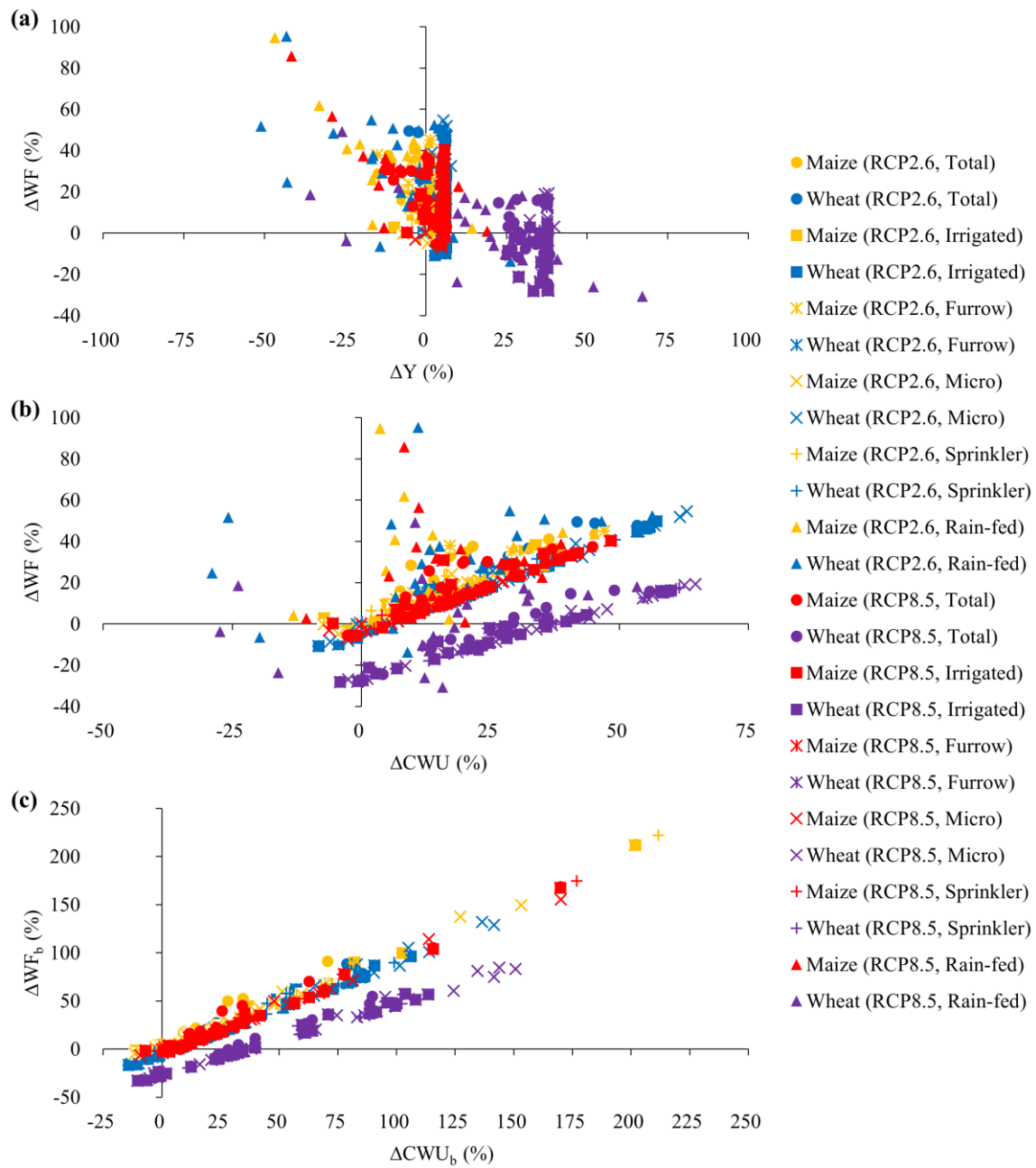


283
 284 **Figure 6.** Spatial distributions in relative changes Δ (%) in WF (bottom left panel) with longitudinal (top panel) and latitudinal (right
 285 panel) changes under different irrigation techniques applied to both crops under two scenarios from 2013 to the 2080s.

286

287 WF is determined by both crop yield (Y) and crop water use (CWU). We compared the relationships between the relative
288 changes in WF (ΔWF) and corresponding Y (ΔY) and CWU (ΔCWU) (Fig. 7). The ΔWF of maize and wheat under future
289 climate change scenarios was inversely proportional to ΔY and directly proportional to ΔCWU . Nevertheless, ΔWF was
290 relatively more sensitive to ΔY . When ΔY was 25 %, ΔWF of wheat under RCP2.6 and maize was approximately -25 %, while
291 ΔWF of wheat under RCP8.5 was approximately -10 %. When ΔCWU was 25 %, ΔWF of wheat under RCP2.6 and maize
292 was ~20 %, while ΔWF of wheat under RCP8.5 was approximately -8 % (Fig. 7a, b). The responses of ΔWF of maize were
293 more sensitive to ΔY and ΔCWU than those of wheat. The responses of ΔWF of maize and wheat under RCP2.6 were more
294 sensitive to ΔY and ΔCWU than those under RCP8.5. Comparison of rain-fed and various irrigation techniques revealed that
295 the correlation between ΔWF and ΔY was stronger for rain-fed crops. For rain-fed maize, R^2 can reach 0.55 (Fig. 7a). ΔWF
296 and ΔCWU were strongly correlated for irrigated crops, and ΔWF and ΔCWU were especially strongly correlated for crops
297 under micro irrigation (R^2 can reach 0.98 for wheat) (Fig. 7b). We also determined the relationship between ΔWF_b and ΔCWU_b ,
298 was similar but more significant than that between ΔWF and ΔCWU (Fig. 7c).

299



300

301 **Figure 7.** Relationships between relative changes Δ (%) in (a) Y and corresponding WF, (b) CWU and corresponding WF, and (c) CWU_b

302

and corresponding WF_b of two crops under RCP2.6 and RCP8.5 from 2013 to the 2080s.

303

304 3.4 Spatiotemporal WF benchmarks responses to climate change

305 Table 2 shows the WF benchmarks of maize and wheat among various irrigation techniques and climate zones in 2013
 306 and future year levels. The WF benchmarks of maize and wheat in the humid zone were 13–32 % higher than those in the arid
 307 zone, which is similar to results obtained by Wang et al. (2019). In the same climate zone, WF benchmarks of wheat were
 308 generally 2–35 % higher than those of maize. However, in the humid zone, the WF benchmark for the 25th production
 309 percentile of maize was 3 % higher than that of wheat under RCP8.5 in the 2080s. In the arid zone, WF benchmarks of rain-
 310 fed maize were 13–34 % higher than those of irrigated maize. In the humid zone of the future, WF benchmarks of rain-fed
 311 wheat were 2–7 % higher than those of irrigated wheat. In general, WF benchmarks of sprinkler-irrigated crops were higher,
 312 while those of micro-irrigated crops were lower. The differences in WF benchmarks among various irrigation techniques were
 313 more significant in the arid zone. WF benchmarks of the crops under micro irrigation were 30–38 % lower than those under
 314 sprinkler irrigation in the arid zone. The difference in the humid zone was only 8–14 %, which is also consistent with the study
 315 by Wang et al. (2019). In the humid zone, however, WF benchmarks of maize under furrow irrigation were 7–21 % higher
 316 than those under sprinkler irrigation.

317

318 **Table 2.** WF benchmarks ($\text{m}^3 \text{t}^{-1}$) of maize and wheat for different climate zones in 2013 and future year levels under two climate change
 319 scenarios in China.

Climate zones	Crop	Type	WF ($\text{m}^3 \text{t}^{-1}$) at different production percentile*					
			20th			25th		
			2013	RCP2.6	RCP8.5	2013	RCP2.6	RCP8.5
Arid	Maize	Total	601	(577, 576, 580)	(589, 584, 566)	623	(661, 658, 655)	(655, 652, 634)
		Irrigated	522	(505, 504, 506)	(503, 503, 496)	548	(508, 507, 511)	(507, 509, 501)
		Furrow	618	(658, 658, 658)	(654, 654, 642)	654	(693, 693, 691)	(689, 687, 674)
		Micro	466	(455, 454, 456)	(456, 454, 440)	477	(459, 458, 460)	(458, 460, 446)
		Sprinkler	700	(727, 725, 723)	(722, 719, 708)	706	(729, 729, 726)	(724, 721, 710)
		Rain-fed	599	(661, 661, 662)	(652, 649, 630)	618	(682, 679, 671)	(672, 667, 652)
	Wheat	Total	753	(776, 764, 781)	(765, 707, 620)	768	(829, 816, 828)	(809, 756, 666)
		Irrigated	754	(776, 764, 781)	(765, 707, 620)	768	(830, 816, 829)	(810, 757, 666)
		Furrow	830	(850, 840, 850)	(830, 774, 680)	940	(885, 875, 887)	(868, 809, 712)
		Micro	648	(701, 690, 705)	(694, 643, 562)	670	(717, 705, 721)	(707, 654, 572)
		Sprinkler	1020	(1003, 998, 1007)	(989, 920, 811)	1032	(1034, 1028, 1038)	(1019, 948, 837)
		Rain-fed	692	(743, 734, 753)	(729, 692, 618)	692	(790, 772, 791)	(769, 737, 653)
Humid	Maize	Total	680	(761, 754, 752)	(756, 752, 739)	718	(813, 807, 807)	(809, 806, 785)
		Irrigated	743	(905, 905, 908)	(902, 900, 881)	782	(939, 939, 944)	(937, 936, 916)
		Furrow	762	(925, 926, 930)	(921, 921, 901)	801	(943, 942, 948)	(940, 939, 919)
		Micro	649	(709, 704, 707)	(694, 696, 683)	660	(734, 726, 732)	(721, 726, 708)
		Sprinkler	713	(770, 771, 768)	(764, 762, 750)	737	(813, 814, 812)	(808, 806, 793)
		Rain-fed	631	(712, 703, 707)	(710, 702, 678)	656	(744, 737, 737)	(740, 736, 716)
	Wheat	Total	873	(933, 932, 946)	(921, 851, 752)	887	(944, 942, 957)	(931, 860, 760)

Irrigated	887	(914, 914, 924)	(900, 841, 744)	897	(925, 926, 937)	(912, 849, 752)
Furrow	887	(914, 914, 925)	(901, 841, 744)	896	(925, 927, 937)	(913, 849, 752)
Micro	820	(821, 826, 838)	(804, 753, 665)	833	(830, 839, 849)	(812, 759, 671)
Sprinkler	933	(949, 944, 955)	(936, 872, 770)	946	(958, 953, 964)	(944, 880, 777)
Rain-fed	812	(973, 958, 984)	(950, 863, 757)	831	(989, 973, 998)	(964, 877, 763)

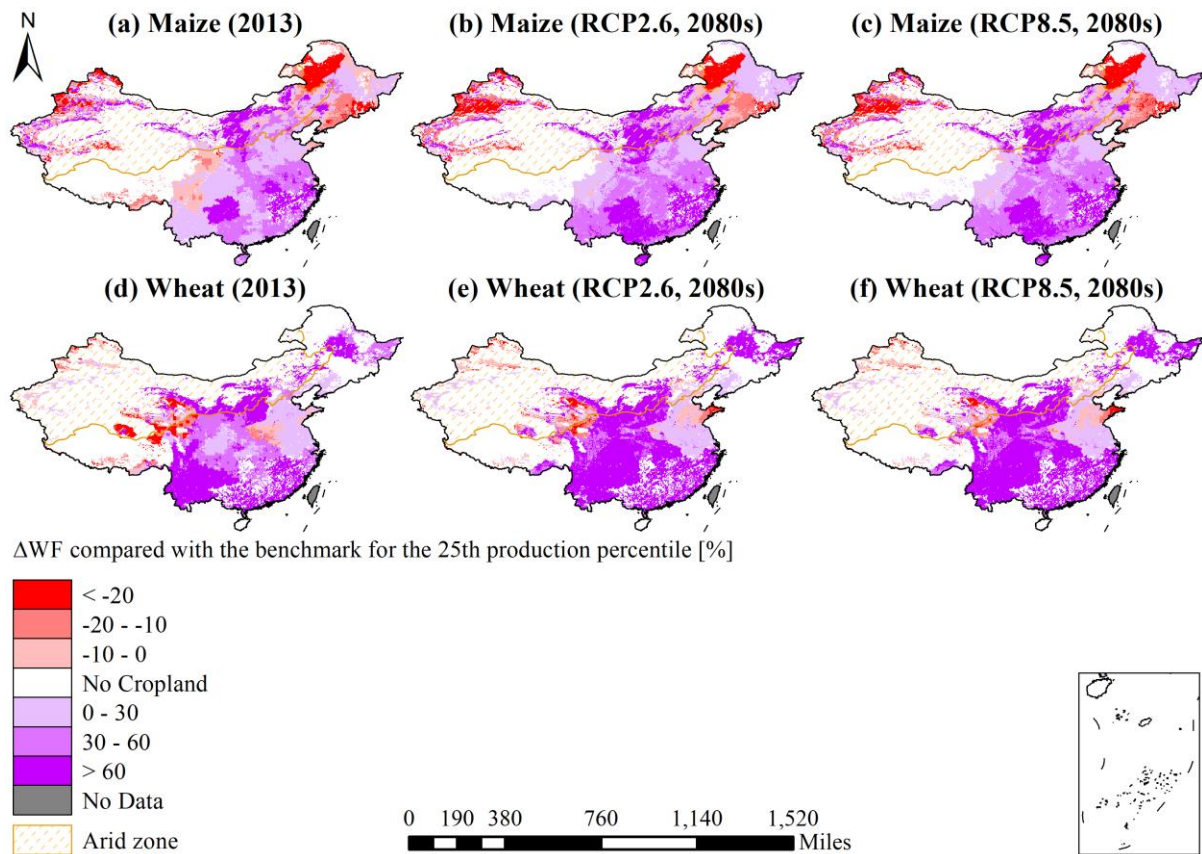
*The three numbers in brackets are the values of 2030s, 2050s and 2080s.

320

321 Compared with the baseline year, 2013, the changes in maize and wheat WF benchmarks under future climate change
322 scenarios are similar to the changes in WF. However, the WF benchmark for the 20th production percentile of maize will
323 decline by 2–6 % in the arid zone. WF benchmarks of wheat under RCP8.5 will decrease by 2–6 % and 13–18 % until the
324 2050s and the 2080s, respectively. The increasing range of the WF benchmark for the 25th production percentile of maize was
325 7–8 % higher in the humid zone than that in the arid zone. The increasing range of the WF benchmark for the 20th production
326 percentile of wheat was 4–5 % higher in the humid zone than that in the arid zone. WF benchmarks of maize and wheat
327 increased to a greater extent under RCP2.6 but decreased to a greater extent under RCP8.5. WF benchmarks of rain-fed crops
328 increased more than those of irrigated crops in the same climate zone. Nevertheless, the increase in WF benchmarks was 7–
329 11 % lower for rain-fed than irrigated maize in the humid zone. WF benchmarks of maize and wheat generally increased
330 relatively more under furrow irrigation and comparatively less under sprinkler irrigation. However, under RCP2.6, the growth
331 rate of the WF benchmark for the 20th production percentile of wheat was 5–6 % higher under micro irrigation than that under
332 furrow irrigation in the arid zone. The increase in the WF benchmark for the 20th production percentile of wheat was 0.19–
333 2 % higher under sprinkler irrigation than that under micro irrigation in the humid zone (Table 2).

334 Figure 8 shows the spatial distribution of the relative changes in the WF of maize and wheat compared with the benchmark
335 for the 25th production percentile in 2013 and the 2080s. In 2013, the WF for 81 % and 79 % of the maize and wheat planted
336 areas, respectively, was higher than its benchmark. The maize planted areas with WF below the benchmark were distributed
337 mainly in Xinjiang in the arid zone and northeast Inner Mongolia in the humid zone (Fig. 8a). The wheat planted areas with
338 WF below the benchmark were distributed mainly in Xinjiang in the arid zone and Qinghai (Fig. 8d). Under future climate
339 change scenarios, the maize and wheat planted areas with the WF below the benchmark will slightly decrease in the 2080s.
340 These areas are mainly distributed in Heilongjiang, Tibet, southern Gansu, and Sichuan in the humid zone for maize; and
341 Henan and Tibet in the humid zone and Qinghai for wheat. This is because that the annual ET_0 will increase relatively faster
342 in Heilongjiang and Tibet, which will lead to a greater increase in WF_b . The annual PR in other regions will significantly
343 increase, which will result in a greater increase in WF_g . Maize and wheat planted areas under RCP8.5 with WF below the
344 benchmark will decrease by 5 % and 4 %, respectively, until the 2080s.

345



346

347 **Figure 8.** Relative changes Δ (%) in the WF of maize and wheat compared with the benchmark for the 25th production percentile in 2013
 348 and the 2080s under RCP2.6 and RCP8.5 in different climate zones of China.

349

350 3.5 Discussion

351 This study analysed and compared the WF and WF benchmarks responses of wheat and maize under rain-fed and various
 352 irrigation conditions and forecasted their responses to future climate change scenarios in China. Under the background that the
 353 annual ET_0 and PR will both increase but ET_0 will increase faster, maize WF will increase under both RCP2.6 and RCP8.5.
 354 Wheat WF will increase under RCP2.6 but decrease under RCP8.5 until the 2080s. Rain-fed crops had higher ranges of
 355 increasing WF, which is consistent with Rosa et al. (2020). The increasing ranges of maize and wheat WF were lowest under
 356 micro irrigation and sprinkler irrigation, respectively. Therefore, the implementation of water-saving irrigation techniques
 357 (micro and sprinkler irrigation) may help mitigate the adverse effects of future climate change on agriculture, which is in line
 358 with Dai et al. (2020). Under future climate change, WF benchmarks will be modified in a manner resembling that for WF.
 359 However, the former changes will not be as significant as the latter in the same area.

360 In 2013, the WF of maize was lower than that of wheat. Nevertheless, maize WF is expected to increase more rapidly
 361 than wheat WF under future climate change scenarios. C4 crops such as maize have higher photosynthetic rates than C3 crops
 362 such as wheat. However, C4 crops are less sensitive to elevated atmospheric CO₂ than C3 crops (Bowes, 1993). Hence, while
 363 maize yield is higher than wheat yield, the former increases less than the latter. We compared current results against those of
 364 previous studies in Table 3. The differences we determined for the relative changes in maize and wheat WF between years and
 365 RCPs resembled those reported by Zhuo et al. (2016d). However, these authors also considered other factors, such as harvested
 366 crop area, technology, diet, and population, that could partially offset the adverse effects of future climate change. Therefore,
 367 maize and wheat WF will decline in the future according to Zhuo et al. (2016d). Fader et al. (2010) studied relative global-
 368 scale changes in maize WF for 2050. Their analysis was conducted in the opposite direction of that of the present study on
 369 China. Moreover, the two studies differed in terms of climate scenario, research area, and crop model. Winter wheat WF in
 370 Germany and Italy will decline by 2050 according to Garofalo et al. (2019). Nevertheless, our research showed that winter
 371 wheat WF will increase in China by 2050. The crop water use in Germany and Italy changes more smaller than that in China.
 372 However, our observed differences in the relative changes in WF between RCPs were consistent with those of Garofalo et al.
 373 (2019); namely, under RCP8.5, WF will either decrease more or increase less.

374

375 **Table 3.** Comparison of the results between current and previous studies.

Reference	Year	Study case	Scenario	Relative changes in WF (%)
Zhuo et al. (2016d)	2030	China Maize	RCP2.6 / RCP8.5	-38–32 / -10–0
		China Wheat		-25–17 / -20–11
	2050	China Maize		-51–43 / -22–8
		China Wheat		-36–27 / -38–27
Current study	2030s (2020–2049)	China Maize	RCP2.6 / RCP8.5	17 / 16
		China Wheat		11 / 9
	2050s (2040–2069)	China Maize		16 / 15
		China Wheat		10 / 0.20
Fader et al. (2010)	2041–2070	Global Maize	SRES A2	-0.44–0.35
Current study	2050s (2040–2069)	China Maize	RCP2.6 / RCP8.5	16 / 15
Garofalo et al. (2019)	2050	Germany Winter wheat	RCP4.5 / RCP8.5	-24 / -26
		Italy Winter wheat		-5 / -6
Current study	2050s (2040–2069)	China Winter wheat	RCP2.6 / RCP8.5	10 / 0.60

376

377 In the future, the spatial distributions of maize and wheat WF will change considerably. By contrast, the spatial
 378 distributions of WF benchmarks will negligibly change. This phenomenon is comparatively more pronounced in the area with
 379 limited agricultural development. In 2013, Guizhou and Guangxi had the highest maize and wheat WF (1,317 m³ t⁻¹ and 3,720
 380 m³ t⁻¹, respectively) (Table S1, S2). In the humid zone, maize WF in Guizhou and wheat WF in Guangxi will increase by 37 %
 381 and 50 %, respectively, under RCP2.6 and by 33 % and 16 %, respectively, under RCP8.5 until the 2080s (Table S5).
 382 Nevertheless, the WF benchmarks for the 25th production percentile of maize and wheat in the humid zone will only increase
 383 by 12 % and 8 %, respectively, under RCP2.6 and increase by 9 % and decrease by 14 %, respectively, under RCP8.5. These

384 areas will nonetheless have great potential for agricultural water conservation in the future. If maize and wheat WF in various
385 regions of China can be reduced to the benchmark for the 25th production percentile, the total CWU can be reduced by 45–66
386 billion m³ (~14–17 %). Rain-fed agriculture can save 27–40 billion m³ (~18–22 %), water which is more than that conserved
387 by irrigation. In irrigated agriculture, furrow irrigation has a comparatively high water-saving potential (17–22 billion m³;
388 ~11–12 %). To optimise the agricultural water-saving potential in China, we must either reduce WF or prevent it from
389 increasing, either by enhancing crop yield or decreasing CWU. However, this goal can only be realised with the support of
390 relevant policies and management practices. The annual PR is relatively low, and the ET₀ is relatively high in North China.
391 Shortage of water for agriculture is a major bottleneck in the development of local agriculture there. However, furrow irrigation
392 is mainly applied in these areas (Fig. S3). Hence, irrigation water use efficiency is low and WF_b is high. High-efficiency,
393 water-saving micro irrigation, and sprinkler irrigation could replace furrow irrigation in these areas so that CWU and WF
394 decrease. The planted areas in the South have abundant precipitation but limited distribution (Fig. S2) and high WF (Fig. 4a,
395 b). WF can be mitigated by implementing ground cover techniques (ex. straw return, mulch) to reduce soil evaporation and by
396 improving farmer skills. WF can also be reduced by optimizing the structure of crop planting. Crops and varieties best adapted
397 to local climate conditions and climate change can lower irrigation requirements and reduce WF.

398 To make climate models comparable and promote their development, The World Climate Research Program (WCRP)
399 has developed and promoted the CMIP since 1995 (Meehl et al., 1997, 2000). Its current iteration is CMIP Phase 6 (CMIP6),
400 which will be used in the forthcoming Intergovernmental Panel on Climate Change's Sixth Assessment Report (IPCC AR6).
401 GCMs and their associated research results based on CMIP5 provided vital support for IPCC's Fifth Assessment Report (IPCC
402 AR5). CMIP5 proposed four RCP scenarios (RCP2.6, RCP4.5, RCP6.0, and RCP8.5) by considering greenhouse gas (GHG)
403 emissions and concentrations, atmospheric pollutant concentrations, and land use in the 21st century (Moss et al., 2008).
404 However, no specific socio-economic assumptions were made. The Scenario Model Intercomparison Project (ScenarioMIP),
405 as the primary activity within CMIP6, will provide a series of new climate scenarios that consider social factors related to
406 climate change adaptation and impacts. They will be based on the combined application of shared socioeconomic pathways
407 (SSPs) and RCPs and will compensate for the limitations of the RCPs in CMIP5 (O'Neill et al., 2016). The climate models in
408 CMIP5 and CMIP6 can both effectively simulate changes in potential evapotranspiration (Liu et al., 2020) and precipitation
409 (Müller et al., 2021) in most parts of the world. Müller et al. (2021) reported that CMIP5 and CMIP6 simulate increasing trends
410 in temperature in a similar fashion. Nevertheless, the simulation generated by CMIP6 is higher than that by CMIP5.
411 Notwithstanding, CMIP5 and CMIP6 are reasonably consistent and similar in terms of their abilities to predict future climate
412 changes. This study focused on the responses of crop production to future climate change. It mainly considered the influences
413 of GHG emission- and concentration-driven climate change and excluded the influences of alterations in socioeconomic
414 development. Therefore, we implemented CMIP5 in our current research.

415 Three are two methods of establishing WF benchmarks (Hoekstra, 2013). Method 1 is based on yield accumulation
416 statistical analysis. Due to the variability of WFs found across regions and among producers within a region, for each crop, we
417 can select the WF of 20 % or 25 % of the producers with the highest water productivity as the WF benchmark (Mekonnen and

418 Hoekstra, 2014). Method 2 is based on the available optimal technique analysis. We can compare the WFs at each location
419 under different agricultural management practices and take the WF associated with optimal practice, which results in the
420 smallest WF, as the WF benchmark (Chukalla et al., 2015). Both methods establish WF benchmarks based on the maximum
421 reasonable water consumption in each step of the product's supply chain (Hoekstra, 2014). Method 1 is suitable for large-scale
422 application. The differences in environmental conditions (such as climate) and development conditions should be considered
423 comprehensively (Mekonnen and Hoekstra, 2014; Zhuo et al., 2016a). The drawback of Method 1 is that no matter what spatial
424 scope one takes in grouping producers, within that scope there will still be variability from place to place even if the differences
425 in regional environmental and development conditions are taken into account (Schyns et al., 2022). Method 2 is suitable for
426 smaller scale and overcomes this drawback of Method 1 to some extent. The Method 2's drawback is that it has the higher
427 requirements on the setting and simulation of different agricultural management practices. We mainly want to explore the
428 response of large-scale WF to future climate change under specific irrigation technique, that is, each irrigation technique has
429 its corresponding WF benchmarks. And only one agricultural management practice, that is irrigation, is considered here.
430 Therefore, we choose Method 1. A combination of methods should be established. If conditions permit, we strongly
431 recommend that Method 1 and Method 2 are combined to establish small-scale WF benchmarks. Different agricultural
432 management practices, such as irrigation, mulching techniques and so on, can be combined to further determine WF
433 benchmarks.

434 The sources of uncertainty in research on the responses of crop production to climate change include GCMs, climate
435 scenarios, crop models, and their interactions (Wang et al., 2020). Semenov and Stratonovitch (2010) proposed that the use of
436 multiple GCMs can reduce the uncertainty associated with them. We selected three GCMs each for wet and dry climate outputs
437 to encompass a broad climate prediction scenario. To objectively and comprehensively project the future climate change trends
438 of China, we selected two extreme RCPs, namely, RCP2.6 and RCP8.5. Wang et al. (2020) suggested that crop models are the
439 main source of uncertainty in predicting wheat yield in China under future climate change. The application of various crop
440 models and parameter settings inevitably lead to different yield forecasts (Asseng et al., 2013). Hence, the use of AquaCrop
441 alone may introduce uncertainty into WF forecasting.

442 The present study had certain limitations in terms of the assumptions it made for the simulation. First, we assumed that
443 the crop parameters (such as planting calendar, HI, and Z_x) for each crop under the identical planting mode (irrigated or rain-
444 fed) were constant on a spatiotemporal scale. Yoon and Choi (2020) proposed that future increases in temperature and
445 precipitation might shorten the crop growth period. Xiao et al. (2020) indicated that the winter wheat and summer maize
446 growing periods will be lengthened and shortened, respectively, under future climate change. However, we did not consider
447 future changes in the crop growth period. Second, we assumed a constant soil surface moisture rate for each grid under the
448 various irrigation techniques. Third, it was assumed that the observed changes in the planted areas in 2013 were based on the
449 2000 raster database, and we ignored the migration of planted areas. Finally, we assumed that the maize and wheat planted
450 areas will not change in the future and would remain consistent with baseline year 2013. Thus, we did not consider future
451 development of cultivated lands.

452 The core content of this study was to quantify the responses of maize and wheat WF and WF benchmarks to future climate
453 change under various irrigation techniques. Future research must improve the accuracy of the crop model simulation and
454 reduce the uncertainty of climate prediction associated with using different GCMs. Moreover, this study only considered future
455 climate change scenarios. Future investigations should also consider the influence of changes in technological development,
456 land use, planting modes, and so on.

457 **4 Conclusions**

458 This study explored the responses of maize and wheat WF accounting and benchmarking to future climate change in
459 China. The crops were subjected to various irrigation techniques. The year 2013 was the baseline, and WF and its benchmarks
460 were quantified for each crop under rain-fed and irrigation (furrow, micro, and sprinkler) management techniques in the 2030s,
461 2050s, and 2080s under RCP2.6 and RCP8.5 at a 5-arc grid scale. The AquaCrop model with the outputs of six GCMs in
462 CMIP5 as its input data was used to simulate the WF of maize and wheat. The results show that: (1) Compared with 2013, the
463 annual ET_0 and PR in the maize and wheat planted areas of China will both increase; however, the former will increase faster
464 than the latter. (2) Maize WF will increase under both RCP2.6 and RCP8.5 by 17 % and 13 %, respectively, until the 2080s.
465 Wheat WF will increase under RCP2.6 (by 12 % until the 2080s) but decrease by 12 % under RCP8.5 until the 2080s. Rain-
466 fed crops were more vulnerable to the adverse impacts of future climate change, and their WF increased to a greater extent
467 than that of irrigated crops. Micro irrigation and sprinkler irrigation resulted in the lowest increases in WF for maize and wheat,
468 respectively. Hence, these water-saving irrigation practices effectively mitigated the negative impact of climate change. (3)
469 Within different climate zones and under various irrigation techniques, there will be significant differences in the responses of
470 WF benchmarks to future climate change. The changes in WF and its benchmarks will be similar in response to future climate
471 change. The rate of increase in WF benchmarks for sprinkler-irrigated crops will generally be lower than those for rain-fed,
472 micro-irrigated, and furrow-irrigated crops within the same climate zone. However, the change in the spatial distribution of
473 WF benchmarks will not be as significant as that of WF itself. Moreover, this difference will be more pronounced in the region
474 with low agricultural development. Additionally, this study also demonstrated that the agricultural water in China still has
475 substantial water-saving potential and can be effectively conserved.

476

477 **Data availability.** Data sources are listed in Sect. 2.5. Data generated in this paper are available by contacting La Zhuo.

478 **Competing interests.** The authors declare that they have no conflict of interest.

479 **Author contribution**

480 La Zhuo and Pute Wu designed the study. Zhiwei Yue and Xiangxiang Ji carried it out, and prepared the manuscript with
481 contributions from all co-authors.

482 **Acknowledgements**

483 The study is financially supported by the Program for Cultivating Outstanding Talents on Agriculture, Ministry of Agriculture
484 and Rural Affairs, People's Republic of China [13210321], and the National Natural Science Foundation of China Grants
485 [51809215].

486

487 **References**

- 488 Ahmadi, M., Etedali, H. R., and Elbeltagi, A.: Evaluation of the effect of climate change on maize water footprint under RCPs
489 scenarios in Qazvin plain, Iran, *Agr. Water Manage.*, 254, 106969, <https://doi.org/10.1016/j.agwat.2021.106969>, 2021.
- 490 Allen, R. G., Pereira, L. S., Raes, D., and Smith, M.: Crop evapotranspiration-Guidelines for computing crop water
491 requirements-FAO Irrigation and drainage paper 56, 300, FAO, Rome, Italy, 1998.
- 492 Arora, V. K., Scinocca, J. F., Boer, G. J., Christian, J. R., Denman, K. L., Flato, G. M., Kharin, V. V., Lee, W. G., and
493 Merryfield, W. J.: Carbon emission limits required to satisfy future representative concentration pathways of greenhouse
494 gases, *Geophys. Res. Lett.*, 38, 387–404, <https://doi.org/10.1029/2010GL046270>, 2011.
- 495 Arunrat, N., Pumijumnong, N., Sreenonchai, S., Chareonwong, U., and Wang, C.: Assessment of climate change impact on
496 rice yield and water footprint of large-scale and individual farming in Thailand, *Sci. Total Environ.*, 726, 137864,
497 <https://doi.org/10.1016/j.scitotenv.2020.137864>, 2020.
- 498 Asseng, S., Ewert, F., Rosenzweig, C., Jones, J. W., Hatfield, J. L., Ruane, A. C., Boote, K. J., Thorburn, P. J., Rötter, R. P.,
499 Cammarano, D., Brisson, N., Basso, B., Martre, P., Aggarwal, P. K., Angulo, C., Bertuzzi, P., Biernath, C., Challinor, A.
500 J., Doltra, J., Gayler, S., Goldberg, R., Grant, R., Heng, L., Hooker, J., Hunt, L. A., Ingwersen, J., Izaurralde, R. C.,
501 Kersebaum, K. C., Müller, C., Naresh Kumar, C., Nendel, C., O'Leary, G., Olesen, J. E., Osborne, T. M., Palosuo, T.,
502 Priesack, E., Ripoche, D., Semenov, M. A., Shcherbak, I., Steduto, P., Stöckle, C., Stratonovitch, P., Streck, T., Supit, I.,
503 Tao, F., Travasso, M., Waha, K., Wallach, D., White, J. W., Williams, J. R., and Wolf, J.: Uncertainty in simulating wheat
504 yields under climate change, *Nat. Clim. Chang.*, 3, 827–832, <https://doi.org/10.1038/nclimate1916>, 2013.
- 505 Bai, T. and Gao, J.: Optimization of the nitrogen fertilizer schedule of maize under drip irrigation in Jilin, China, based on
506 DSSAT and GA, *Agric Water Manag.*, 244, 106555, <https://doi.org/10.1016/j.agwat.2020.106555>, 2021.
- 507 Batjes, N.: ISRIC-WISE Derived Soil Properties on a 5 by 5 Arc-Minutes Global Grid (Ver. 1.2), ISRIC, Wageningen, The
508 Netherlands, available at: <https://www.isric.org>, 2012.

509 Bowes, G.: Facing the Inevitable: Plants and Increasing Atmospheric CO₂, *Annu. Rev. Plant Phys. Plant Mol. Biol.*, 44, 309–
510 332, <https://doi.org/10.1146/annurev.pp.44.060193.001521>, 1993.

511 CCAFS: CCAFS-Climate Statistically Downscaled Delta Method data, Climate Change, Agriculture and Food Security,
512 available at: www.ccafs-climate.org, 2015.

513 CIDDC: China Irrigation and Drainage Development Center, China, available at:
514 <http://www.jsdg.com.cn/temp/Index/Display.asp?NewsID=12313>, last access: 14 April 2022.

515 CEDA: Climatic Research Unit (CRU) time-series datasets of variations in climate with variations in other phenomena, NCAS
516 British Atmospheric Data Centre, date of citation, available at: <http://catalogue.ceda.ac.uk/uuid>, 2018.

517 Chukalla, A. D., Krol, M. S., and Hoekstra, A. Y.: Green and blue water footprint reduction in irrigated agriculture: Effect of
518 irrigation techniques irrigation strategies and mulching, *Hydrol. Earth Syst. Sci.*, 19, 4877–4891,
519 <https://doi.org/10.5194/hess-19-4877-2015>, 2015.

520 Dai, C., Qin, X. S., Lu, W. T., and Huang, Y.: Assessing adaptation measures on agricultural water productivity under climate
521 change: A case study of Huai River Basin, China, *Sci. Total Environ.*, 721, 137777,
522 <https://doi.org/10.1016/j.scitotenv.2020.137777>, 2020.

523 Delworth, T. L., Broccoli, A. J., Rosati, A., Stouffer, R. J., Balaji, V., Beesley, J. A., Cooke, W. F., Dixon, K. W., Dunne, J.,
524 Dunne, K. A., Durachta, J. W., Findell, K. L., Ginoux, P., Gnanadesikan, A., Gordon, C. T., Griffies, S. M., Gudgel, R.,
525 Harrison, M. J., Held, I. M., Hemler, R. S., Horowitz, L. W., Klein, S. A., Knutson, T. R., Kushner, P. J., Langenhorst,
526 A. R., Lee, H. C., Lin, S. J., Lu, J., Malyshev, S. L., Milly, P. C. D., Ramaswamy, V., Russell, J., Schwarzkopf, M. D.,
527 Shevliakova, E., Sirutis, J. J., Spelman, M. J., Stern, W. F., Winton, M., Wittenberg, A. T., Wyman, B., Zeng, F., and
528 Zhang, R.: GFDL’s CM2 Global Coupled Climate Models. Part I: Formulation and Simulation Characteristics, *J. Clim.*,
529 19, 643–674, <https://doi.org/10.1175/JCLI3629.1>, 2006.

530 Dijkshoorn, J. A., Engelen, V. W. P. V., and Huting, J. R. M.: Soil and landform properties for LADA partner countries
531 (Argentina, China, Cuba, Senegal, South Africa and Tunisia), ISRIC–World Soil Information and FAO, Wageningen, the
532 Netherlands, available at: <https://www.isric.org/>, <https://doi.org/10.13031/2013.42676>, 2008.

533 Donner, L. J., Wyman, B. L., Hemler, R. S., Horowitz, L. W., Ming, Y., Zhao, M., Golaz, J. C., Ginoux, P., Lin, S. J.,
534 Schwarzkopf, M. D., Austin, J., Alaka, G., Cooke, W. F., Delworth, T. L., Freidenreich, S. M., Gordon, C. T., Griffies,
535 S. M., Held, I. M., Hurlin, W. J., Klein, S. A., Knutson, T. R., Langenhorst, A. R., Lee, H. C., Lin, Y., Magi, B. I.,
536 Malyshev, S. L., Milly, P. C. D., Naik, V., Nath, M. J., Pincus, R., Ploshay, J. J., Ramaswamy, V., Seman, C. J.,
537 Shevliakova, E., Sirutis, J. J., Stern, W. F., Stouffer, R. J., Wilson, R. J., Winton, M., Wittenberg, A. T., and Zeng, F.:
538 The Dynamical Core, Physical Parameterizations, and Basic Simulation Characteristics of the Atmospheric Component
539 AM3 of the GFDL Global Coupled Model CM3, *J. Clim.*, 24, 3484–3519, <https://doi.org/10.1175/2011JCLI3955.1>, 2011.

540 Dufresne, J. L., Foujols, M. A., Denvil, S., Caubel, A., Marti, O., Aumont, O., Balkanski, Y., Bekki, S., Bellenger, H., Benschila,
541 R., Bony, S., Bopp, L., Braconnot, P., Brockmann, P., Cadule, P., Cheruy, F., Codron, F., Cozic, A., Cugnet, D., Noblet,
542 N. D., Duvel, J. P., Ethé, C., Fairhead, L., Fichefet, T., Flavoni, S., Friedlingstein, P., Grandpeix, J. Y., Guez, L., Guilyardi,

543 E., Hauglustaine, D., Hourdin, F., Idelkadi, A., Ghattas, J., Joussaume, S., Kageyama, M., Krinner, G., Labetoulle, S.,
544 Lahellec, A., Lefebvre, M. P., Lefevre, F., Levy, C., Li, Z. X., Lloyd, J., Lott, F., Madec, G., Mancip, M., Marchand, M.,
545 Masson, S., Meurdesoif, Y., Mignot, J., Musat, I., Parouty, S., Polcher, J., Rio, C., Schulz, M., Swingedouw, D., Szopa,
546 S., Talandier, C., Terray, P., Viovy, N., and Vuichard, N.: Climate change projections using the IPSL-CM5 Earth System
547 Model: from CMIP3 to CMIP5, *Clim. Dyn.*, 40, 2123–2165, <https://doi.org/10.1007/s00382-012-1636-1>, 2013.

548 Fader, M., Rost, S., Müller, C., Bondeau, A., and Gerten, D.: Virtual water content of temperate cereals and maize: Present
549 and potential future patterns, *J. Hydrol.*, 384, 218–231, <https://doi.org/10.1016/j.jhydrol.2009.12.011>, 2010.

550 FAO: FAOSTAT on-line database, Food and Agriculture Organization of the United Nation, Rome, Italy, available at:
551 <http://www.fao.org/faostat/en/#data/QC>, 2021.

552 Garofalo, P., Ventrella, D., Kersebaum, K. C., Gobin, A., Trnka, M., Giglio, L., Dubrovský, M., and Castellini, M.: Water
553 footprint of winter wheat under climate change: Trends and uncertainties associated to the ensemble of crop models, *Sci.*
554 *Total Environ.*, 658, 1186–1208, <https://doi.org/10.1016/j.scitotenv.2018.12.279>, 2019.

555 Guo, H., Li, S., Wong, F. L., Qin, S., Wang, Y., Yang, D., and Lam, H. M.: Drivers of carbon flux in drip irrigation maize
556 fields in northwest China, *Carbon Balance Manag.*, 16, 12, <https://doi.org/10.1186/s13021-021-00176-5>, 2021.

557 Harris, I., Jones, P. D., Osborn, T. J., and Lister, D. H.: Updated high-resolution grids of monthly climatic observations - the
558 CRU TS3.10 Dataset, *Int. J. Climatol.*, 34, 623–642, <https://doi.org/10.1002/joc.3711>, 2014.

559 Hatfield, J. L. and Dold, C.: Water-Use Efficiency: Advances and Challenges in a Changing Climate, *Front. Plant Sci.*, 10,
560 103, <https://doi.org/10.3389/fpls.2019.00103>, 2019.

561 Hoekstra, A. Y. (ed.): Virtual water trade: Proceedings of the International Expert Meeting on Virtual Water Trade, Delft, the
562 Netherlands, 12–13 December 2002, Value of Water Research Report Series No. 12, UNESCO-IHE, Delft, The
563 Netherlands, 2003.

564 Hoekstra, A. Y.: The water footprint of modern consumer society, Routledge, London, UK, 208 pp, 2013.

565 Hoekstra, A. Y.: Sustainable, efficient, and equitable water use: the three pillars under wise freshwater allocation, *WIREs*
566 *Water*, 1, 31–40, <https://doi.org/10.1002/wat2.1000>, 2014.

567 Hoekstra, A. Y., Chapagain, A. K., Aldaya, M. M., and Mekonnen, M. M.: The Water Footprint Assessment Manual: Setting
568 the Global Standard, Earthscan, London, UK, 2011.

569 Hurrell, J. W., Holland, M. M., Gent, P. R., Ghan, S., Kay, J. E., Kushner, P. J., Lamarque, J. F., Large, W. G., Lawrence, D.,
570 Lindsay, K., Lipscomb, W. H., Long, M. C., Mahowald, M., Marsh, D. R., Neale, R. B., Rasch, P., Vavrus, S., Vertenstein,
571 M., Bader, D., Collins, W. D., Hack, J. J., Kiehl, J., and Marshall, S.: The Community Earth System Model: A Framework
572 for Collaborative Research, *Bull. Am. Meteorol. Soc.*, 94, 1339–1360, <https://doi.org/10.1175/BAMS-D-12-00121.1>,
573 2013.

574 IPCC: Summary for Policymakers. In: Climate Change 2021: The Physical Science Basis. Contribution of Working Group I
575 to the Sixth Assessment Report of the Intergovernmental Panel on Climate Change, edited by: Masson-Delmotte, V.,
576 Zhai, P., Pirani, A., Connors, S. L., Péan, C., Berger, S., Caud, N., Chen, Y., Goldfarb, L., Gomis, M. L., Huang, M.,

577 Leitzell, K., Lonnoy, E., Matthews, J. B. R., Maycock, T. K., Waterfield, T., Yelekçi, O., Yu, R., and Zhou, B., Cambridge
578 University Press, In Press, 2021.

579 Jans, Y., Bloh, W. V., Schaphoff, S., and Müller, C.: Global cotton production under climate change – Implications for yield
580 and water consumption, *Hydrol. Earth Syst. Sci.*, 25, 2027–2044, <https://doi.org/10.5194/hess-25-2027-2021>, 2021.

581 Kappelle, M.: WMO Statement on the State of the Global Climate in 2019, World Meteorological Organization, Geneva,
582 Switzerland, 2020.

583 Konapala, G., Mishra, A. K., Wada, Y., and Mann, M. E.: Climate change will affect global water availability through
584 compounding changes in seasonal precipitation and evaporation, *Nat. Commun.*, 11, 3044,
585 <https://doi.org/10.1038/s41467-020-16757-w>, 2020.

586 Li, H., Mei, X., Nangia, V., Guo, R., Liu, Y., Hao, W., and Wang, J.: Effects of different nitrogen fertilizers on the yield,
587 water- and nitrogen-use efficiencies of drip-fertigated wheat and maize in the North China Plain, *Agric Water Manag.*,
588 243, 106474, <https://doi.org/10.1016/j.agwat.2020.106474>, 2021.

589 Liu, X., Li, C., Zhao, T., and Han, L.: Future changes of global potential evapotranspiration simulated from CMIP5 to CMIP6
590 models, *Atmos. Oceanic Sci Lett.*, 13, 568–575, <https://doi.org/10.1080/16742834.2020.1824983>, 2020.

591 Lobell, D. B. and Gourdjji, S. M.: The influence of climate change on global crop productivity, *Plant Physiol.*, 160, 1686–1697,
592 <https://doi.org/10.1104/pp.112.208298>, 2012.

593 Mali, S. S., Shirsath, P. B., and Islam, A.: A high-resolution assessment of climate change impact on water footprints of cereal
594 production in India, *Sci. Rep.*, 11, 8715, <https://doi.org/10.1038/s41598-021-88223-6>, 2021.

595 Meehl, G. A., Boer, G. J., Covey, C., Latif, M., and Stouffer, R. J.: Intercomparison makes for a better climate model, *Eos.*
596 *Trans. Amer. Geophys. Union*, 78, 445–451, <https://doi.org/10.1029/97EO00276>, 1997.

597 Meehl, G. A., Boer, G. J., Covey, C., Latif, M., and Stouffer, R. J.: The Coupled Model Intercomparison Project (CMIP), *Bull.*
598 *Am. Meteorol. Soc.*, 81, 313–318, [https://doi.org/10.1175/1520-0477\(2000\)081<0313:TCMIPC>2.3.CO;2](https://doi.org/10.1175/1520-0477(2000)081<0313:TCMIPC>2.3.CO;2), 2000.

599 Mekonnen, M. M. and Hoekstra, A. Y.: A global and high-resolution assessment of the green, blue and grey water footprint
600 of wheat, *Hydrol. Earth Syst. Sci.*, 14, 1259–1276, <https://doi.org/10.5194/hess-14-1259-2010>, 2010.

601 Mekonnen, M. M. and Hoekstra, A. Y.: The green, blue and grey water footprint of crops and derived crop products, *Hydrol.*
602 *Earth Syst. Sci.*, 15, 1577-1600, <https://doi.org/10.5194/hess-15-1577-2011>, 2011.

603 Mekonnen, M. M. and Hoekstra, A. Y.: Water footprint benchmarks for crop production: A first global assessment, *Ecol.*
604 *Indic.*, 46, 214–223, <https://doi.org/10.1016/j.ecolind.2014.06.013>, 2014.

605 Mialyk, O., Schyns, J. F., Booij, M. J., and Hogeboom, R. J.: Historical simulation of maize water footprints with a new global
606 gridded crop model ACEA, *Hydrol. Earth Syst. Sci.*, 26, 923–940, <https://doi.org/10.5194/hess-26-923-2022>, 2022.

607 Middleton, N. and Thomas, D. S. G.: World atlas of desertification, Arnold, London, UK, 1997.

608 Moss, R., Babiker, M., Brinkman, S., Calvo, E., Carter, T., Edmonds, J., Elgizouli, I., Emori, S., Erda, L., Hibbard, K., Jones,
609 R., Kainuma, M., Kelleher, J., Lamarque, J. F., Manning, M., Matthews, B., Meehl, J., Meyer, L., Mitchell, J.,
610 Nakicenovic, N., O'Neill, B., Pichs, R., Riahi, K., Rose, S., Runci, P., Stouffer, R., van Vuuren, D., Weyant, J., Wilbanks,

611 T., van Ypersele, J. P., and Zurek, M.: Towards New Scenarios for Analysis of Emissions, Climate Change, Impacts, and
612 Response Strategies, IPCC Expert Meeting Report, 19–21 September, 2007, Noordwijkerhout, Netherlands,
613 Intergovernmental Panel on Climate Change (IPCC), Geneva, Switzerland, 132 pp, 2008.

614 Müller, C., Franke, J., Jägermeyr, J., Ruane, A. C., Elliott, J., Moyer, E., Heinke, J., Falloon, P. D., Folberth, C., Francois, L.,
615 Hank, T., César Izaurralde, R., Jacquemin, I., Liu, W., Olin, S., Pugh, T. A. M., Williams, K., and Zabel, F.: Exploring
616 uncertainties in global crop yield projections in a large ensemble of crop models and CMIP5 and CMIP6 climate scenarios,
617 *Environ. Res. Lett.*, 16, 034040, <https://doi.org/10.1088/1748-9326/abd8fc>, 2021.

618 Myers, S. S., Smith, M. R., Guth, S., Golden, C. D., Vaitla, B., Mueller, N. D., Dangour, A. D., and Huybers, P.: Climate
619 Change and Global Food Systems: Potential Impacts on Food Security and Undernutrition, *Annu. Rev. Public Health*, 38,
620 259–277, <https://doi.org/10.1146/annurev-publhealth-031816-044356>, 2017.

621 Navarro-Racines, C., Tarapues, J., Thornton, P., Jarvis, A., and Ramirez-Villegas, J.: High-resolution and bias-corrected
622 CMIP5 projections for climate change impact assessments, *Sci. Data*, 7, 7, <https://doi.org/10.1038/s41597-019-0343-8>,
623 2020.

624 NBSC: National Data, China, National Bureau of Statistics, Beijing, China, available at: <https://data.stats.gov.cn/>, 2021.

625 NOAA: National Oceanic and Atmospheric Administration, U.S, available at: <https://www.esrl.noaa.gov>, 2018.

626 O’Neill, B. C., Tebaldi, C., van Vuuren, D. P., Eyring, V., Friedlingstein, P., Hurtt, G., Hurtt, R., Kriegler, E., Lamarque, J.
627 F., Lowe, J., Meehl, G. A., Moss, R., Riahi, K., and Sanderson, B. M.: The Scenario Model Intercomparison Project
628 (ScenarioMIP) for CMIP6, *Geosci. Model Dev.*, 9, 3461–3482, <https://doi.org/10.5194/gmd-9-3461-2016>, 2016.

629 Pastor, A. V., Palazzo, A., Havlik, P., Biemans, H., Wada, Y., Obersteiner, M., Kabat, P., and Ludwig, F.: The global nexus
630 of food–trade–water sustaining environmental flows by 2050, *Nat. Sustain.*, 2, 499–507, [https://doi.org/10.1038/s41893-
631 019-0287-1](https://doi.org/10.1038/s41893-019-0287-1), 2019.

632 Portmann, F. T., Siebert, S., and Döll, P.: MIRCA2000-Global monthly irrigated and rainfed crop areas around the year 2000:
633 A new high-resolution data set for agricultural and hydrological modelling, *Global Biogeochem. Cy.*, 24,
634 <https://doi.org/10.1029/2008gb003435>, 2010.

635 Qiao, F., Song, Z., Bao, Y., Song, Y., Shu, Q., Huang, C., and Zhao, W.: Development and evaluation of an Earth System
636 Model with surface gravity waves, *J. Geophys. Res. Ocean.*, 118, 4514–4524, <https://doi.org/10.1002/jgrc.20327>, 2013.

637 Raes, D., Steduto, P., Hsiao, T. C., and Fereres, E.: Reference manual, Chapter 2, AquaCrop model, Version 6.0, Food and
638 Agriculture Organization of the United Nations, Rome, Italy, 2017.

639 Rallison, R. E.: Origin and evolution of the SCS runoff equation, in: Symposium on Watershed Management, Boise, Idaho,
640 United States, 21–23 July, 912–924, 1980.

641 Riahi, K., Gruebler, A., and Nakicenovic, N.: Scenarios of long-term socio-economic and environmental development under
642 climate stabilization, *Technol. Forecast. Soc. Chang.*, 74, 887–935, <https://doi.org/10.1016/j.techfore.2006.05.026>, 2007.

643 Rosa, L., Chiarelli, D. D., Sangiorgio, M., Beltran-Peña, A. A., Rulli, M. C., D’Odorico, P., and Fung, I.: Potential for
644 sustainable irrigation expansion in a 3° C warmer climate, *Proc. Natl. Acad. Sci. U. S. A.*, 117, 29526–29534,
645 <https://doi.org/10.1073/pnas.2017796117>, 2020.

646 Schmidt, G. A., Kelley, M., Nazarenko, L., Ruedy, R., Russell, G. L., Aleinov, I., Bauer, M., Bauer, S. E., Bhat, M. K., Bleck,
647 R., Canuto, V., Chen, Y. H., Cheng, Y., Clune, T. L., Genio, A. D., Fainchtein, R. D., Faluvegi, G., Hansen, J. E., Healy,
648 R. J., Kiang, N. Y., Koch, D., Lacis, A. A., LeGrande, A. N., Lerner, J., Lo, K. K., Matthews, E. E., Menon, S., Miller,
649 R. L., Oinas, V., Olosó, A. O., Perlwitz, J. P., Puma, M. J., Putman, W. M., Rind, D., Romanou, A., Sato, M., Shindell,
650 D. T., Sun, S., Syed, R. A., Tausnev, N., Tsigaridis, K., Unger, N., Voulgarakis, A., Yao, M. S., and Zhang, J.:
651 Configuration and assessment of the GISS ModelE2 contributions to the CMIP5 archive, *J. Adv. Model. Earth Syst.*, 6,
652 141–184, <https://doi.org/10.1002/2013MS000265>, 2014.

653 Schmidt, G. A., Ruedy, R., Hansen, J. E., Aleinov, I., Bell, N., Bauer, M., Bauer, S., Cairns, B., Canuto, V., Cheng, Y.,
654 Delgenio, A. D., Faluvegi, G., Friend, A. D., Hall, T. M., Hu, Y., Kelley, M., Kiang, N. Y., Koch, D., Lacis, A. A., Lerner,
655 J., Lo, K. K., Miller, R. L., Nazarenko, L., Oinas, V., Perlwitz, J., Perlwitz, J., Rind, D., Romanou, A., Russell, G. L.,
656 Sato, M., Shindell, D. T., Stone, P. H., Sun, S., Tausnev, N., Thresher, D., and Yao, M. S.: Present-Day Atmospheric
657 Simulations Using GISS ModelE: Comparison to In Situ, Satellite, and Reanalysis Data, *J. Clim.*, 19, 153–192,
658 <https://doi.org/10.1175/JCLI3612.1>, 2006.

659 Schyns, J. F., Hogeboom, R. J., and Krol, M. S.: 4 - Water Footprint Assessment: towards water-wise food systems, in: *Food*
660 *Systems Modelling*, edited by: Peters, C., and Thilmany, D., Academic Press, Salt Lake City, USA, 63–88,
661 <https://doi.org/10.1016/B978-0-12-822112-9.00006-0>, 2022.

662 Semenov, M. A. and Stratonovitch, P.: Use of multi-model ensembles from global climate models for assessment of climate
663 change impacts, *Clim. Res.*, 41, 1–14, <https://doi.org/10.3354/cr00836>, 2010.

664 Tian, Y., Ruth, M., Zhu, D., Ding, J., and Morris, N.: A Sustainability Assessment of Five Major Food Crops' Water Footprints
665 in China from 1978 to 2010, *Sustainability*, 11, 1–20, <https://doi.org/10.3390/su11216179>, 2019.

666 Trnka, M., Feng, S., Semenov, M. A., Olesen, J. E., Kersebaum, K. C., Rötter, R. P., Semerádová, D., Klem, K., Huang, W.,
667 Ruiz-Ramos, M., Hlavinka, P., Meitner, J., Balek, J., Havlík, P., and Büntgen, U.: Mitigation efforts will not fully alleviate
668 the increase in water scarcity occurrence probability in wheat-producing areas, *Sci. Adv.*, 5, eaau2406,
669 <https://doi.org/10.1126/sciadv.aau2406>, 2019.

670 USDA: Estimation of direct runoff from storm rainfall, Section 4 Hydrology, Chapter 4, *National Engineering Handbook*,
671 Washington DC, USA, 1–24, 1964.

672 van Vuuren, D. P., den Elzen, M. G. J., Lucas, P. L., Eickhout, B., Strengers, B. J., van Ruijven, B., Wonink, S., and van Houdt,
673 R.: Stabilizing greenhouse gas concentrations at low levels: an assessment of reduction strategies and costs, *Clim. Change*,
674 81, 119–159, <https://doi.org/10.1007/s10584-006-9172-9>, 2007.

675 von Salzen, K., Scinocca, J. F., McFarlane, N. A., Li, J., Cole, J. N. S., Plummer, D., Verseghy, D., Reader, M. C., Ma, X.,
676 Lazare, M., and Solheim, L.: The Canadian Fourth Generation Atmospheric Global Climate Model (CanAM4). Part I:

677 Representation of Physical Processes, *Atmosphere-Ocean*, 51, 104–125, <https://doi.org/10.1080/07055900.2012.755610>,
678 2013.

679 Wang, B., Feng, P., Liu, D. L., O’Leary, G. J., Macadam, I., Waters, C., Asseng, S., Cowie, A., Jiang, T., Xiao, D., Ruan, H.,
680 He, J., and Yu, Q.: Sources of uncertainty for wheat yield projections under future climate are site-specific, *Nat. Food.*,
681 1, 720–728, <https://doi.org/10.1038/s43016-020-00181-w>, 2020.

682 Wang, C., Guo, L., Li, Y., and Wang, Z.: Systematic Comparison of C3 and C4 Plants Based on Metabolic Network Analysis,
683 *BMC Syst Biol.*, 6, S9, <https://doi.org/10.1186/1752-0509-6-S2-S9>, 2012.

684 Wang, J., Gao, S., Xu, Y., and Wang, H.: Application and Existing Problems of Drip Irrigation for Wheat in Xinjiang, in: 2011
685 International Conference on Agricultural and Natural Resources Engineering (ANRE 2011), Intelligent Information
686 Technology Application Association, Singapore, 3 July 2011, 25–29, 2011.

687 Wang, W., Zhuo, L., Li, M., Liu, Y., and Wu, P.: The Effect of Development in Water-Saving Irrigation Techniques on Spatial-
688 Temporal Variations in Crop Water Footprint and Benchmarking, *J. Hydrol.*, 577, 123916,
689 <https://doi.org/10.1016/j.jhydrol.2019.123916>, 2019.

690 Xiao, D., Liu, D. L., Wang, B., Feng, P., Bai, H., and Tang, J.: Climate change impact on yields and water use of wheat and
691 maize in the North China Plain under future climate change scenarios, *Agr. Water Manage.*, 238, 106238, 2020.

692 Xu, Z., Chen, X., Wu, S. R., Gong, M., Du, Y., Wang, J., Li, Y., and Liu, J.: Spatial-temporal assessment of water footprint,
693 water scarcity and crop water productivity in a major crop production region, *J. Clean. Prod.*, 224, 375–383,
694 <https://doi.org/10.1016/j.jclepro.2019.03.108>, 2019.

695 Yoon, P. R. and Choi, J. Y.: Effects of shift in growing season due to climate change on rice yield and crop water requirements,
696 *Paddy Water Environ.*, 18, 291–307, <https://doi.org/10.1007/s10333-019-00782-7>, 2020.

697 Zain, M., Si, Z., Chen, J., Mehmood, F., Rahman, S. U., Shah, A. N., Li, S., Gao, Y., and Duan, A.: Suitable nitrogen
698 application mode and lateral spacing for drip-irrigated winter wheat in North China Plain, *PLoS One*,
699 <https://doi.org/10.1371/journal.pone.0260008>, 2021.

700 Zheng, J., Wang, W., Ding, Y., Liu, G., Xing, W., Cao, X., and Chen, D.: Assessment of climate change impact on the water
701 footprint in rice production: Historical simulation and future projections at two representative rice cropping sites of China,
702 *Sci. Total Environ.*, 709, 136190, <https://doi.org/10.1016/j.scitotenv.2019.136190>, 2020.

703 Zhuo, L., Liu, Y., Yang, H., Hoekstra, A. Y., Liu, W., Cao, X., Wang, M., and Wu, P.: Water for maize for pigs for pork: An
704 analysis of inter-provincial trade in China, *Water Res.*, 166, 115074, <https://doi.org/10.1016/j.watres.2019.115074>, 2019.

705 Zhuo, L., Mekonnen, M. M., and Hoekstra, A. Y.: Sensitivity and uncertainty in crop water footprint accounting: a case study
706 for the Yellow River basin, *Hydrol. Earth Syst. Sci.*, 18, 2219–2234, <https://doi.org/10.5194/hess-18-2219-2014>, 2014.

707 Zhuo, L., Mekonnen, M. M., and Hoekstra, A. Y.: Benchmark levels for the consumptive water footprint of crop production
708 for different environmental conditions: a case study for winter wheat in China, *Hydrol. Earth Syst. Sci.*, 20, 4547–4559,
709 <https://doi.org/10.5194/hess-20-4547-2016>, 2016a.

710 Zhuo, L., Mekonnen, M. M., Hoekstra, A. Y., and Wada, Y.: Inter- and intra-annual variation of water footprint of crops and
711 blue water scarcity in the Yellow River basin (1961–2009), *Adv. Water Resour.*, 87, 29–41,
712 <https://doi.org/10.1016/j.advwatres.2015.11.002>, 2016b.

713 Zhuo, L., Mekonnen, M. M., and Hoekstra, A. Y.: The effect of inter-annual variability of consumption, production, trade and
714 climate on crop-related green and blue water footprints and inter-regional virtual water trade: A study for China (1978-
715 2008), *Water Res.*, 94, 73–85, <https://doi.org/10.1016/j.watres.2016.02.037>, 2016c.

716 Zhuo, L., Mekonnen, M. M., and Hoekstra, A. Y.: Consumptive water footprint and virtual water trade scenarios for China —
717 With a focus on crop production, consumption and trade, *Environ. Int.*, 94, 211–223,
718 <https://doi.org/10.1016/j.envint.2016.05.019>, 2016d.